

# EUROPEAN Journal of Medicine



Has been issued since 2013.  
ISSN 2308-6513. E-ISSN 2310-3434  
2017. 5(2). Issued 2 times a year

## EDITORIAL BOARD

**Bykov Anatolii** – Kuban State Medical University, Krasnodar, Russian Federation (Editor-in-Chief)

**Anisimov Vladimir** – FSI N.N. Petrov Research Institute of Oncology of Rosmedtechnology, Saint-Petersburg, Russian Federation

**Khodasevich Leonid** – Sochi State University, Sochi, Russian Federation

**Goncharova Nadezhda** – Research Institute of Medical Primatology, Sochi, Russian Federation

**Gordon Kirill** – Kuban State Medical University, Krasnodar, Russian Federation

**Goswami Sribas** – Serampore College, West Bengal, India

**Gurovich Isaak** – Moscow Research Institute of Psychiatry, Moscow, Russian Federation

**Manilal Aseer** – Arba Minch University, Ethiopia

**Ovechkin Denis** – Sumy State University, Sumy, Ukraine

**Pogorielov Maksym** – Sumy State University, Sumy, Ukraine

**Razvodovsky Yuri** – Grodno State Medical University, Grodno, Belarus

**Rehman Fazal ur** – Aligarh Muslim University, India

**Ryazantseva Natal'ya** – Siberian State Medical University, Tomsk, Russian Federation

**Semiglazov Vladimir** – FSI N.N. Petrov Research Institute of Oncology of Rosmedtechnology, Saint-Petersburg, Russian Federation

**Semiglazov Vladislav** – First Pavlov State Medical University of St. Peterburg, Saint-Petersburg, Russian Federation

**Shah Syed Imran Ali** – Hammersmith Hospital, Department of Surgery and Cancer, London, United Kingdom

**Shihabuddeen Ismail TM** – Yenepoya Medical College, Yenepoya University, Mangalore, India

**Titov Vladimir** – Cardiology Research Complex MH RF, Moscow, Russian Federation

**Zaridze David** – Federal State Budgetary Scientific Institution «N.N. Blokhin Russian Cancer Research Center», Moscow, Russian Federation

Journal is indexed by: **CAS Source Index** (USA), **CiteFactor** (Canada), **CrossRef** (UK), **EBSCOhost Electronic Journals Service** (USA), **Electronic scientific library** (Russia), **Journal Index** (USA), **Open Academic Journals Index** (Russia), **ResearchBib** (Japan), **Sherpa Romeo** (Spain), **ULRICH's WEB** (USA).

All manuscripts are peer reviewed by experts in the respective field. Authors of the manuscripts bear responsibility for their content, credibility and reliability.

Editorial board doesn't expect the manuscripts' authors to always agree with its opinion.

Postal Address: 1367/4, Stara Vajnorska str., Bratislava – Nove Mesto, Slovakia, 831 04  
Release date 16.09.17.  
Format 21 × 29,7/4.

Website: <http://ejournal5.com/>  
E-mail: [ejm2013@mail.ru](mailto:ejm2013@mail.ru)  
Headset Georgia.

Founder and Editor: Academic Publishing House Researcher s.r.o. Order № 16.

© European Journal of Medicine, 2017

European Journal of Medicine

2017

Is.

2

C O N T E N T S

**Articles and Statements**

Biophysical Research of ZEOLITH detox and ZEOLITH Creme of the Company L. Vitae, I. Ignatov .....	31
Research with Model Systems in Biophysics and Biochemistry of Bioinfluence of Dimitar Risimanski I. Ignatov .....	43
Action of Cytisinum on the Transport Mediators and Calcium Channel of Glutamatergic Neurotransmitter Systems of the NMDA Receptor N.N. Khoshimov, K.E. Nasirov .....	56

Copyright © 2017 by Academic Publishing House Researcher s.r.o.



Published in the Slovak Republic  
European Journal of Medicine  
Has been issued since 2013.  
ISSN: 2308-6513  
E-ISSN: 2310-3434  
2017, 5(2): 31-42

DOI: 10.13187/ejm.2017.2.31  
[www.ejournal5.com](http://www.ejournal5.com)



## Biophysical Research of ZEOLITH detox and ZEOLITH Creme of the Company

Lava Vitae <sup>a</sup>, Ignat Ignatov <sup>a, \*</sup>

<sup>a</sup> Scientific Research Center of Medical Biophysics, Sofia, Bulgaria

### Abstract

We studied the mathematical model of interaction with water of natural mineral and microporous crystalline mineral ZEOLITH detox and ZEOLITH Creme of LavaVitae Company (Austria). In this report are submitted data about the interaction of ZEOLITH detox and ZEOLITH Crème with water, obtained by non-equilibrium (NES) and differential-equilibrium energy spectrum (DNES) of water. The average energy ( $\Delta E_{H...O}$ ) of hydrogen H...O-bonds among individual molecules H<sub>2</sub>O after treatment of ZEOLITH detox with water measured by NES- and DNES-methods is  $\Delta E = -0.0034 \pm 0.0011$  eV for ZEOLITH detox. The average energy ( $\Delta E_{H...O}$ ) of hydrogen H...O-bonds among individual molecules H<sub>2</sub>O after treatment of ZEOLITH detox with water measured by NES- and DNES-methods is  $\Delta E = -0.0034 \pm 0.0011$  eV for ZEOLITH detox. The average energy ( $\Delta E_{H...O}$ ) of hydrogen H...O-bonds among individual molecules H<sub>2</sub>O after treatment of ZEOLITH detox with water measured by NES- and DNES-methods is  $\Delta E = -0.007 \pm 0.0011$  eV for ZEOLITH Creme. These results suggest the restructuring of  $\Delta E_{H...O}$  values among H<sub>2</sub>O molecules with a statistically reliable increase of local extremums in DNES-spectra. The research is performed for ZEOLITH detox with study of pH and oxidative reduction potential (ORP).

**Keywords:** ZEOLITH detox, ZEOLITH Crème, nanostructures, mathematical model, NES, DNES.

### 1. Introduction

The ZEOLITH detox is mineral refers to new generation of natural mineral sorbents (NMS). Zeolites are the aluminosilicate members of the family of microporous solids known as "molecular sieves", named by their ability to selectively sort molecules based primarily on a size exclusion process. Natural zeolites form when volcanic rocks and ash layers react with alkaline groundwater. Zeolites also crystallize in post-depositional environments over periods ranging from thousands to millions of years in shallow marine basins. Naturally occurring zeolites are rarely pure and are contaminated to varying degrees by other minerals, metals, quarts, or other zeolites. For this reason, naturally occurring zeolites are excluded from many important commercial applications where uniformity and purity are essentials.

As natural mineral zeolite has unusually broad scope of application in industry. Adsorption, catalytic, and reduction-oxidation Zeolites is widely used in industry as a desiccant of gases and

\* Corresponding author  
E-mail addresses: [mbioph@dir.bg](mailto:mbioph@dir.bg) (I. Ignatov)

liquids, for treatment of drinking and sewage water from heavy metals, ammonia, phosphorus, as catalyst in petrochemical industry for benzene extraction, for production of detergents and for extracting of radionuclides in nuclear reprocessing. It is also used in medicine as nutritional supplements having antioxidant properties. Some authors make qualifications of zeolites as nano materials.

A wide range of properties of zeolite defines the search for new areas of industrial application of these minerals in science and nano technology that contributes to a deeper study the mechanism of interaction of these minerals with water. The company LavaVitae produces ZEOLITH Creme with exceptional results on the skin and skin diseases. This paper deals with evaluating of mathematical models of interaction of ZEOLITH detox and ZEOLITH Creme with water.

## **2. Materials and Methods**

### **2.1. Materials**

The study is performed with samples of ZEOLITH detox ZEOLITH Creme from LavaVitae Company.

**There are valid the following methods for research of zeolite.**

### **2.2. Analytical Methods**

The analytical methods were accredited by the Institute of Geology of Ore Deposits. Petrography, Mineralogy, and Geochemistry (Russian Academy of Sciences). Samples were treated by various methods as ICP-OES, GC, and SEM.

### **2.3. Gas-Chromatography**

Gas-chromatography (GC) is performed at Main Testing Centre of Drinking Water (Moscow, the Russian Federation) on Kristall 4000 LUX M using Chromaton AW-DMCS and Inerton-DMCS columns (stationary phases 5% SE-30 and 5% OV-17), equipped with flame ionization detector (FID) and using helium (He) as a carrier gas.

### **2.4. Inductively Coupled Plasma Optical Emission Spectrometry (ICP-OES)**

The mineral composition is studied by inductively coupled plasma optical emission spectrometry (ICP-OES) on Agilent ICP 710-OES (Agilent Technologies, USA) spectrometer, equipped with plasma atomizer (under argon stream), MegaPixel CCD detector, and 40 MHz free-running, air-cooled RF generator, and Computer-optimized exhale system: the spectral range at 167–785 nm; plasma gas: 0–22.5 l/min in 1.5 l/min; power output: 700–1500 W in 50 W increments.

### **2.5. Transmission Electron Microscopy (TEM)**

The structural studies were carried out with using JSM 35 CF (JEOL Ltd., Korea) device, equipped with X-ray microanalyzer “Tracor Northern TN”, SE detector, thermomolecular pump, and tungsten electron gun (Harpin type W filament, DC heating); working pressure:  $10^{-4}$  Pa ( $10^{-6}$  Torr); magnification: 300.000, resolution: 3.0 nm, accelerating voltage: 1–30 kV; sample size: 60–130 mm.

### **2.6. IR-Spectroscopy**

IR-spectra of water samples, obtained after being contacted 3 days with shungite and zeolite, are registered on Fourier-IR spectrometer Bruker Vertex (“Bruker”, Germany) (a spectral range: average IR – 370–7800  $\text{cm}^{-1}$ ; visible – 2500–8000  $\text{cm}^{-1}$ ; the permission – 0.5  $\text{cm}^{-1}$ ; accuracy of wave number – 0.1  $\text{cm}^{-1}$  on 2000  $\text{cm}^{-1}$ );

**For the research of ZEOLITH detox and ZEOLITH Creme the methods are:**

### **2.7. Non-equilibrium Spectrum (NES) and Differential Non-equilibrium Spectrum (DNES)**

The energy spectrum of water is characterized by a non-equilibrium process of water droplets evaporation, therefore, the term non-equilibrium spectrum (NES) of water is used. The difference  $\Delta f(E) = f(\text{samples of water}) - f(\text{control sample of water})$  – is called the “differential non-equilibrium energy spectrum of water” (DNES).

### **2.8. Measurement of pH and ORP (oxidative-redox potential)**

The research is performed from Georgi Gluhchev with device from Hanna Instruments.

## **3. Results and Discussion**

In comparison with zeolite comprises a microporous crystalline aluminosilicate mineral commonly used as commercial adsorbents, three-dimensional framework of which is formed by linking via the vertices the tetrahedral  $[\text{AlO}_4]^{2-}$  and  $[\text{SiO}_4]^{2-}$  (Panayotova, Velikov, 2002). Each

tetrahedron  $[\text{AlO}_4]^{2-}$  creates a negative charge of the carcasses compensated by cations ( $\text{H}^+$ ,  $\text{Na}^+$ ,  $\text{K}^+$ ,  $\text{Ca}^{2+}$ ,  $\text{NH}_4^+$ , etc.), in most cases, capable of cation exchange in solutions. Tetrahedrons formed the secondary structural units, such as six-membered rings, five-membered rings, truncated octahedra, etc. Zeolites framework comprise interacting channels and cavities forming a porous structure with a pore size of 0.3–1.0 nm. Average crystal size of the zeolites may range from 0.5 to 30  $\mu\text{m}$ .

By the measurement of IR spectra in the range of vibrations in the crystal mineral framework one can obtain the information: a) on the structure of the framework, particularly type lattice ratio  $\text{SiO}_2/\text{Al}_2\text{O}_3$ , nature and location of cations and changes in the structure in the process of the thermal treatment; b) on the nature of the surface of the structural groups, which often serve as adsorption and catalytically active sites.

Other method for obtaining information about the average energy of hydrogen bonds in an aqueous sample is measuring of the spectrum of the water state. It was established experimentally that at evaporation of water droplet the contact angle  $\theta$  decreases discretely to zero, whereas the diameter of the droplet changes insignificantly (Antonov, 1995). By measuring this angle within a regular time intervals a functional dependence  $f(\theta)$  can be determined, which is designated by the spectrum of the water state (Ignatov, 2005; Ignatov, 2012; Ignatov, Mosin, 2013). For practical purposes by registering the spectrum of water state it is possible to obtain information about the averaged energy of hydrogen bonds in an aqueous sample. For this purpose the model of W. Luck was used, which consider water as an associated liquid, consisted of  $\text{O}-\text{H}\dots\text{O}-\text{H}$  groups (Luck et al., 1980). The major part of these groups is designated by the energy of hydrogen bonds ( $-E$ ), while the others are free ( $E = 0$ ). The energy distribution function  $f(E)$  is measured in electron-volts ( $\text{eV}^{-1}$ ) and may be varied under the influence of various external factors on water as temperature and pressure.

For calculation of the function  $f(E)$  experimental dependence between the water surface tension measured by the wetting angle ( $\theta$ ) and the energy of hydrogen bonds ( $E$ ) is established:

$$f(E) = b f(\theta) / 1 - (1 + b E)^2)^{1/2},$$

where  $b = 14.33 \text{ eV}^{-1}$ ;  $\theta = \arcsin(-1 - b E)$

The energy of hydrogen bonds ( $E$ ) measured in electron-volts ( $\text{eV}$ ) is designated by the spectrum of energy distribution. This spectrum is characterized by non-equilibrium process of water droplets evaporation, thus the term “non-equilibrium energy spectrum of water” (NES) is applied.

The difference  $\Delta f(E) = f(\text{samples of water}) - f(\text{control sample of water})$  – is designated the “differential non-equilibrium energy spectrum of water” (DNES).

DNES is calculated in milli-electron volts (0.001  $\text{eV}$  or  $\text{meV}$ ) is a measure of changes in the structure of water as a result of external factors. The cumulative effect of all other factors is the same for the control sample of water and the water sample, which is under the influence of this impact. The research with NES method of water drops received after 3 days stay with zeolite in deionized water may also give valuable information on the possible number of hydrogen bonds as percent of water molecules with different values of distribution of energies. These distributions are basically connected with restructuring of  $\text{H}_2\text{O}$  molecules with the same energies.

### **3.1. Results with spectral analysis of 1% solution of ZEOLITH detox**

The average energy ( $E_{\text{H}\dots\text{O}}$ ) of hydrogen  $\text{H}\dots\text{O}$ -bonds among individual  $\text{H}_2\text{O}$  molecules in 1 % solution of ZEOLITH detox is measured at  $E = -0.1219 \text{ eV}$ . The result for the control sample (deionized water) is  $E = -0.1185 \text{ eV}$ . The results obtained with the NES method are recalculated with the DNES method as a difference of the NES (1 % solution of ZEOLITH detox) minus the NES (control sample with deionized water) equalled the DNES spectrum of 1 % solution of ZEOLITH detox. Thus, the result for 1 % solution of ZEOLITH detox recalculated with the DNES method is  $\Delta E = -0.0034 \pm 0.0011 \text{ eV}$ . The result shows the increasing of the values of the energy of hydrogen bonds in 1 % solution of ZEOLITH detox regarding the deionized water. The result is effect of stimulation on human body. This shows restructuring of water molecules in configurations of clusters, which influence usefully on human health on molecular and cellular level. The effects are describing with mathematical model of 1 % solution of ZEOLITH detox.

### 3.2. Mathematical model of ZEOLITH detox

The research with the NES method of water drops is received with 1 % solution ZEOLITH detox, and deionized water as control sample. The mathematical models of 1 % solution ZEOLITH detox gives the valuable information for the possible number of hydrogen bonds as percent of H<sub>2</sub>O molecules with different values of distribution of energies (Table 1 and Fig. 1). These distributions are basically connected with the restructuring of H<sub>2</sub>O molecules having the same energies.

**Table 1.** The distribution (% , (-E<sub>value</sub>)/(-E<sub>total value</sub>) of H<sub>2</sub>O molecules in 1 % water solution of ZEOLITH detox (product of LavaVitae, Austria) and control deionized water

-E(eV) x-axis	1 % water solution ZEOLITH detox (LavaVitae) y-axis (%((-E <sub>value</sub> )* / (-E <sub>total value</sub> )) <sup>**</sup>	Control Sample Deionized water y-axis (%((- E <sub>value</sub> )* / (- E <sub>total value</sub> )) <sup>**</sup>	-E(eV) x-axis	1 % water solution ZEOLITH detox (LavaVitae) y-axis (%((-E <sub>value</sub> )* / (-E <sub>total value</sub> )) <sup>**</sup>	Control Sample Deionized water y-axis (%((-E <sub>value</sub> )* / -E <sub>total value</sub> ) <sup>**</sup>
0.0937	0	6.7	0.1187	0	15.5
0.0962	0	6.7	0.1212	<b>18.9<sup>2</sup></b>	0
0.0987	0	6.7	0.1237	0	6.7
0.1012	6.0	15.5	0.1262	0	6.7
0.1037	12.5	6.7	0.1287	0	0
0.1062	0	6.7	0.1312	0	3.3
0.1087	3.1	0	0.1337	12.5	0
0.1112	<b>3.1<sup>1</sup></b>	0	0.1362	12.5	3.3
0.1137	0	15.5	0.1387	<b>18.9<sup>3</sup></b>	0
0.1162	12.5	0	–	–	–

Notes:

E=-0.1212 eV is the local extremum for anti inflammatory effect

E= -0.1387 eV is the local extremum for inhibition of development of tumor cells of molecular level

Notes:

\* The result (-E<sub>value</sub>) is the result of hydrogen bonds energy for one parameter of (-E)

\*\* The result (-E<sub>value</sub>) is the total result of hydrogen bonds energy

Figure 1 shows the distribution (% , (-E<sub>value</sub>)/(-E<sub>total value</sub>) of H<sub>2</sub>O molecules in and 1 % of water solution of ZEOLITH detox (product of LavaVitae, Austria) (red line) and control sample deionized water (blue line).

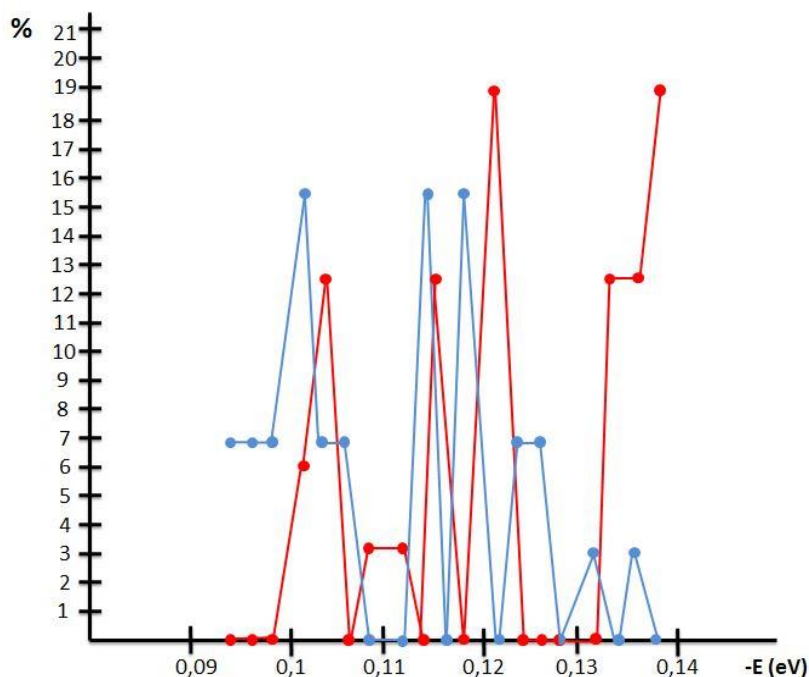


**Fig. 1.** Mathematical model (Ignatov, Mosin, 2013) of 1 % water solution of ZEOLITH detox (product of LavaVitae, Austria)

Notes:

$E = -0.1212$  eV is the local extremum for anti-inflammatory effect

$E = -0.1387$  eV is the local extremum for inhibition of development of tumor cells of molecular level

The experimental data obtained testified the following conclusions from the mathematical model of in 1 % water solution of ZEOLITH detox (product of LavaVitae, Austria) and control deionized water. The distribution ( $\%$ ,  $(-E_{\text{value}})/(-E_{\text{total value}})$ ) of water molecules in mathematical model of in 1 % water solution of ZEOLITH detox (product of LavaVitae, Austria) and control deionized water. The distribution ( $\%$ ,  $(-E_{\text{value}})/(-E_{\text{total value}})$ ) of water molecules in ZEOLITH detox (product of LavaVitae, Austria) according control sample is different. However, for the value  $E = -0.1387$  eV or  $\lambda = 8.95$   $\mu\text{m}$  there is the biggest local extremum (18.9 ( $\%$ ,  $(-E_{\text{value}})/(-E_{\text{total value}})$ )) corresponding to the restructuring of hydrogen bonds among  $\text{H}_2\text{O}$  molecules for inhibition of development of tumor cells of molecular level. This difference may indicate on the different number of hydrogen bonds in water samples, as well as their physical parameters (pH, ORP), resulting in different distribution of  $\text{H}_2\text{O}$  molecules and different values of  $\text{H}_2\text{O}$  molecules with ratios of  $(-E_{\text{value}})/(-E_{\text{total value}})$ . Particularly it was observed the statistical re-structuring of  $\text{H}_2\text{O}$  molecules in water samples according to the energies. The experimental data may prove that stipulates the restructuring of  $\text{H}_2\text{O}$  molecules on molecular level and may be used for the prophylaxis of development of tumor cells. For the value  $E = -0.1212$  eV or  $\lambda = 10.23$   $\mu\text{m}$  there is the bigger local extremum (18.9 ( $\%$ ,  $(-E_{\text{value}})/(-E_{\text{total value}})$ )) corresponding to the restructuring of hydrogen bonds among  $\text{H}_2\text{O}$  molecules for anti-inflammatory effect.. The experimental data for ZEOLITH detox may prove that stipulates the restructuring of  $\text{H}_2\text{O}$  molecules on molecular level and the biophysical effects are:

$E = -0.1212$  eV is the local extremum for anti-inflammatory effect

$E = -0.1387$  eV is the local extremum for inhibition of development of tumor cells of molecular level

### 3.3. Results with spectral analysis of 1% solution of ZEOLITH Creme

The average energy ( $E_{\text{H...O}}$ ) of hydrogen H...O-bonds among individual  $\text{H}_2\text{O}$  molecules in 1 % solution of ZEOLITH Creme is measured at  $E = -0.1200$  eV. The result for the control sample (deionized water) is  $E = -0.1130$  eV. The results obtained with the NES method are recalculated with the DNES method as a difference of the NES (1 % solution of ZEOLITH Creme) minus the NES (control sample with deionized water) equaled the DNES spectrum of 1 % solution of ZEOLITH

Creme. Thus, the result for 1 % solution of ZEOLITH Creme recalculated with the DNES method is  $\Delta E = -0.007 \pm 0.0011$  eV. The result shows the increasing of the values of the energy of hydrogen bonds in 1 % solution of ZEOLITH detox regarding the deionized water. The results is effect of stimulation on human body. The result is 6.4 times more than statistical reliable result. This shows restructuring of water molecules in configurations of clusters, which influence usefully on human health on molecular and cellular level. The effects are describing with mathematical model of 1 % solution of ZEOLITH Creme.

**3.2. Mathematical model of ZEOLITH detox**

The research with the NES method of water drops is received with 1 % solutions ZEOLITH Creme and deionized water as control samples. The mathematical models of 1 % solution ZEOLITH Creme give the valuable information for the possible number of hydrogen bonds as percent of H<sub>2</sub>O molecules with different values of distribution of energies (Table 1). These distributions are basically connected with the restructuring of H<sub>2</sub>O molecules having the same energies.

**3.3. Mathematical model of ZEOLITH Creme (product of the company LavaVitae)**

The research with the NES method of water drops is received with 1 % solution ZEOLITH Creme, and deionized water as control sample. The mathematical model of 1 % solution ZEOLITH Creme gives the valuable information for the possible number of hydrogen bonds as percent of H<sub>2</sub>O molecules with different values of distribution of energies (Table 2 and Fig. 2). These distributions are basically connected with the restructuring of H<sub>2</sub>O molecules having the same energies.

**Table 2.** The distribution (% , (-E<sub>value</sub>)/(-E<sub>totalvalue</sub>)) of H<sub>2</sub>O molecules in 1 % water solution of ZEOLITH Creme (product of LavaVitae, Austria) and control deionized water

-E(eV) x-axis	1 % water solution ZEOLITH Creme (LavaVitae) y-axis (%((-E <sub>value</sub> )* / (-E <sub>total value</sub> ))**	Control Sample Deionized water y-axis (%((-E <sub>value</sub> )* / (-E <sub>total value</sub> ))**	-E(eV) x-axis	1 % water solution ZEOLITH Creme (LavaVitae) y-axis (%((-E <sub>value</sub> )* / (-E <sub>total value</sub> ))**	Control Sample Deionized water y-axis (%((-E <sub>value</sub> )* / (-E <sub>total value</sub> ))**
0.0937	0	0	0.1187	0	5.7
0.0962	0	11.4	0.1212	<b>15.2<sup>2</sup></b>	5.7
0.0987	7.8	5.7	0.1237	3.8	0
0.1012	7.8	5.7	0.1262	3.8	5.7
0.1037	3.8	11.4	0.1287	7.7	5.7
0.1062	7.8	11.4	0.1312	7.7	0
0.1087	3.8	0	0.1337	7.7	0
0.1112	<b>3.8<sup>1</sup></b>	5.7	0.1362	3.8	5.7
0.1137	0	8.8	0.1387	<b>7.7<sup>3</sup></b>	5.7
0.1162	7.8	5.7	-	-	-

Notes:

E=-0.1212 eV is the local extremum for anti-inflammatory effect

Notes:

\* The result (-E<sub>value</sub>) is the result of hydrogen bonds energy for one parameter of (-E)

\*\* The result (-E<sub>value</sub>) is the total result of hydrogen bonds energy

Figure 2 shows the distribution (% , (-E<sub>value</sub>)/(-E<sub>total value</sub>)) of H<sub>2</sub>O molecules in and 1 % of water solution of ZEOLITH Creme (product of LavaVitae, Austria) (red line) and control sample deionized water (blue line).



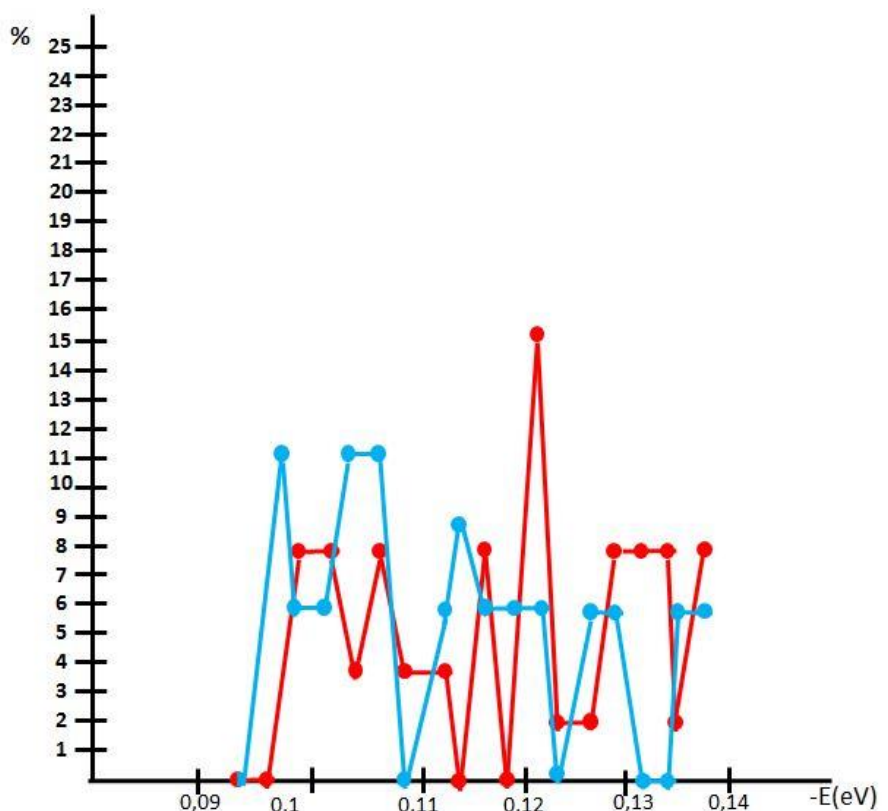


**Fig. 2.** Mathematical model (Ignatov, Mosin, 2013) of 1% water solution of ZEOLITH Creme (product of LavaVitae, Austria).

Notes:

$E = -0.1212$  eV is the local extremum for anti-inflammatory effect

The experimental data obtained testified the following conclusions from the mathematical model of in 1% water solution of ZEOLITH Creme (product of LavaVitae, Austria) and control deionized water. The distribution ( $\%$ ,  $(-E_{\text{value}})/(-E_{\text{total value}})$ ) of water molecules in mathematical model of in 1% water solution of ZEOLITH Creme (product of LavaVitae, Austria) and control deionized water. The distribution ( $\%$ ,  $(-E_{\text{value}})/(-E_{\text{total value}})$ ) of water molecules in ZEOLITH Creme (product of LavaVitae, Austria) according control sample is different. However, for the value  $E = -0.1212$  eV or  $\lambda = 10.23$   $\mu\text{m}$  there is the biggest local extremum (15.2%,  $(-E_{\text{value}})/(-E_{\text{total value}})$ ) corresponding to the restructuring of hydrogen bonds among  $\text{H}_2\text{O}$  molecules for inhibition of development of tumor cells of molecular level. This difference may indicate on the different number of hydrogen bonds in water samples, resulting in different distribution of  $\text{H}_2\text{O}$  molecules and different values of  $\text{H}_2\text{O}$  molecules with ratios of  $(-E_{\text{value}})/(-E_{\text{total value}})$ . Particularly it was observed the statistical re-structuring of  $\text{H}_2\text{O}$  molecules in water samples according to the energies. The experimental data may prove that stipulates the restructuring of  $\text{H}_2\text{O}$  molecules on molecular level and may be used for cleaning of skin with anti-inflammatory effect. The experimental data for ZEOLITH Crème may prove that stipulates the restructuring of  $\text{H}_2\text{O}$  molecules on molecular level and the biophysical effect is:

$E = -0.1212$  eV is the local extremum for anti-inflammatory effect

#### 4. Results with pH and ORP

There are valid the following results of pH as indicator for acid alkaline medium of the products of Lava Vitae. There are the results also of ORP or Oxidation-reduction potential.

The results are for 1% of solutions of products, which are made from deionized water. This research is performed with Georgi Gluhchev from Bulgarian Academy of Science. The results of pH of deionized water is 6.05 and of ORP is 119.7. Table 3 shows the results of pH and ORP.

**Table 3.** Results of products of company LavaVitae for pH and ORP

Product	pH	ORP (mV)	Coordinates Fig. 2
VITA Intense	4.07±0.02	-104.5	Point 1 (4,07; -104.5)
BOOST	3.60±0.02	+113.6	Point 2 (3,90;113.6)
ZEOLITH detox	8.01±0.02	+109.5	Point 3 (8,01;103.3)
Deionized water	6.05±0.02	+119.7	

Figure 3 shows the dependence between the acidity and basicity (pH) of electrochemically activated solutions and the oxidation-reduction potential (ORP). The pH value within the interval from 3 to 10 units and the ORP within the interval from -400 mV to +900 mV characterize the area of the biosphere of microorganisms. Outside these ranges of pH and ORP the microorganisms will hardly survive.

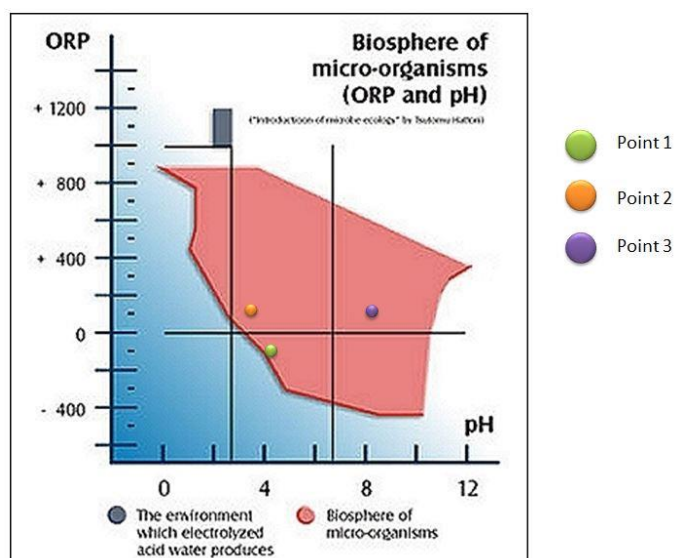


**Fig. 3.** The dependence between acidity and basicity (pH) of solutions and the ORP on the biosphere of micro-organisms (point 1; VITA intense), (point 2; BOOST), point 3; ZEOLITH detox).

Owing to the unique porous structure the mineral Zeolites are ideal absorbents and fillers (Gorshteyn et al., 1979), and as sorbents have a number of positive characteristics:

- High adsorption capacity, characterized by low resistance to water pressure;
- Mechanical strength and low abrasion resistance;
- Corrosion-resistance;
- Absorption capacity relatives to many substances, both organic (oil, benzene, phenol, pesticides, etc.) and inorganic (chlorine, ammonia, heavy metals);
- Catalytic activity;
- Relatively low cost;
- Environmental friendliness and ecological safety.

## 5. Discussion and Conclusions

### 5.1. ZEOLITH detox (product of LavaVitae company)

The interaction of ZEOLITH detox with water is quiet complex and results the restructuring

of energy values among H<sub>2</sub>O molecules with a statistically reliable increase of local extremums in DNES-spectra after treatment of ZEOLITH detox with water. These values are measured at -0.1219 eV for ZEOLITH detox. The result for control sample (deionized water) is -0.1185 eV. The results with NES method were recalculated by the DNES method. The result of ZEOLITH detox with DNES method is  $0.0034 \pm 0.0011$  eV.

From the NES and DNES spectrum and mathematical model of 1 % solution of ZEOLITH detox and deionized water as control sample are valid the following conclusions for biophysical effects for ZEOLITH detox (LavaVitae Company)

- Anti-inflammatory effect;
- inhibition of development of tumor cells of molecular level;

Naturally occurring zeolites are rarely pure and are contaminated to varying degrees by other minerals, metals, quarts, or other zeolites. For this reason, naturally occurring zeolites are excluded from many important commercial applications where uniformity and purity are essential. In comparison with zeolite comprises a microporous crystalline aluminosilicate mineral commonly used as adsorbent. Zeolite creates a negative charge of the carcasses compensated by cations (H<sup>+</sup>, Na<sup>+</sup>, K<sup>+</sup>, Ca<sup>2+</sup>, NH<sub>4</sub><sup>+</sup>, etc.), in most cases, capable of cations exchange in solutions. Efficiency of using zeolite is stipulated by the high range of valuable properties (absorption, catalytic, antioxidant, regenerative, antibacterial). There is permanent antioxidant activity of zeolite on enzymes (Dogliotti et al., 2012; Ignatov, Mosin, 2015).

### 5.2. ZEOLITH Creme (product of LavaVitae company)

From the NES and DNES spectrum and mathematical model of 1% solution of ZEOLITH Crème and deionized water as control sample is valid the following conclusion for biophysical effects for ZEOLITH Creme (LavaVitae company)

- anti-inflammatory effect;

Naturally occurring zeolites are rarely pure and are contaminated to varying degrees by other minerals, metals, quarts, or other zeolites. For this reason, naturally occurring zeolites are excluded from many important commercial applications where uniformity and purity are essential. In comparison with zeolite comprises a microporous crystalline aluminosilicate mineral commonly used as adsorbent. Zeolite creates negative charge of the carcasses compensated by cations (H<sup>+</sup>, Na<sup>+</sup>, K<sup>+</sup>, Ca<sup>2+</sup>, NH<sub>4</sub><sup>+</sup>, etc.), in most cases, capable of cations exchange in solutions. Efficiency of using zeolite is stipulated by the high range of valuable properties (absorption, catalytic, antioxidant, regenerative, antibacterial). There is permanent antioxidant activity of zeolite on enzymes (Dogliotti et al., 2012; Ignatov, Mosin, 2015).

## 6. Acknowledgements

The author wish to thank to Georgi Gluhchev for the research of pH and ORP. The author express thankful to Teodora Todorova for the preparation of the figures.

## References

- Antonov, 1995 – Antonov, A. (1995). Research of the Nonequilibrium Processes in the Area in Allocated Systems. Diss. Thesis Doctor of Physical Sciences. Sofia: Blagoevgrad: pp. 1–255.
- Gluhchev et al., 2015a – Gluhchev, G., Ignatov, I., Karadzhov, S., Miloshev, G., Ivanov, I., Mosin, O.V. (2015). Biocidal Effects of Electrochemically Activated Water. *Journal of Health, Medicine and Nursing*, V. 11, pp. 67-83.
- Gluhchev et al., 2015b – Gluhchev, G., Ignatov, I., Karadzhov, S., Miloshev, G., Ivanov, N., Mosin, O.V. (2015). Electrochemically Activated Water: Biophysical and Biological Effects of Anolyte and Catholyte Types of Water. *European Journal of Molecular Biotechnology*, V.1, pp. 12-26.
- Gluhchev et al., 2015c – Gluhchev, G., Ignatov, I., Karadzhov, S., Miloshev, G., Ivanov, N., Mosin, O.V. (2015). Studying the Antimicrobial and Antiviral Effects of Electrochemically Activated NaCl Solutions of Anolyte and Catholyte on a Strain of E. Coli DH5 and Classical Swine Fever (CSF) Virus. *European Journal of Medicine*, 9 (3), pp. 124-138.
- Gluhchev et al., 2015d – Gluhchev, G., Ignatov, I., Karadzhov, S., Miloshev, G., Ivanov, I., Mosin, O.V. (2015). Electrochemically Activated Water. Biophysical and Biological Effects of Anolyte and Catholyte as Types of Water. *Journal of Medicine, Physiology and Biophysics*, Vol. 10, pp. 1-17.

[Gluhchev et al., 2015e](#) – Gluhchev, G., Ignatov, I., Karadzhov, S., Miloshev, G., Ivanov, I., Mosin, O. V. (2015). Studying of Virucidal and Biocidal Effects of Electrochemically Activated Anolyte and Catholyte Types of Water on Classical Swine Fever Virus (CSF) and Bacterium E. coli DH5. *Journal of Medicine, Physiology and Biophysics*, Vol. 13, pp. 1-17.

[Ignatov et al., 2014a](#) – Ignatov, I., Karadzhov, S., Atanasov, A., Ivanova, E., Mosin, O. V. (2014). Electrochemical Aqueous Sodium Chloride Solution (Anolyte and Catholyte) as Types of Water. Mathematical Models. Study of Effects of Anolyte on the Virus of Classical Swine Fever Virus. *Journal of Health, Medicine and Nursing*, Vol. 8, pp. 1-28.

[Ignatov et al., 2014b](#) – Ignatov, I., Mosin, O. V., Bauer, E. (2014). Carbonaceous Fullerene Mineral Shungite and Aluminosilicate Mineral Zeolite. Mathematical Model and Practical Application of Water Solution of Water Shungite and Zeolite. *Journal of Medicine, Physiology and Biophysics*, Vol. 4, pp. 27-44.

[Ignatov et al., 2015](#) – Ignatov, I., Mosin, O.V., Gluhchev, G., Karadzhov, S., Miloshev, G., Ivanov, N. (2015). The Evaluation of Mathematical Model of Interaction of Electrochemically Activated Water Solutions (Anolyte and Catholyte) with Water. *European Reviews of Chemical Research*, Vol. 2 (4), pp. 72-86.

[Ignatov et al., 2015a](#) – Ignatov, I., Gluhchev, G., Karadzhov, S., Miloshev, G., Ivanov, I., Mosin, O. V. (2015). Preparation of Electrochemically Activated Water Solutions (Catholyte/Anolyte) and Studying of their Physical-Chemical Properties. *Journal of Medicine, Physiology and Biophysics*, Vol. 13, pp. 18-38.

[Ignatov et al., 2015b](#) – Ignatov, I., Gluhchev, G., Karadzhov, S., Miloshev, G., Ivanov, I., Mosin, O. V. (2015). Preparation of Electrochemically Activated Water Solutions (Catholyte/Anolyte) and Studying of their Physical-Chemical Properties. *Journal of Health, Medicine and Nursing*, Vol. 13, pp. 64-78.

[Ignatov et al., 2015c](#) – Ignatov, I., Mosin, O. V., Gluhchev, G., Karadzhov, S., Miloshev, G., Ivanov, I., (2015). Studying Electrochemically Activated NaCl Solutions of Anolyte and Catholyte by Methods of Non-Equilibrium Energy Spectrum (NES) and Differential Non-Equilibrium Energy Spectrum (DNES). *Journal of Medicine, Physiology and Biophysics*, Vol. 14, pp. 6-18.

[Ignatov et al., 2015d](#) – Ignatov, I., Gluhchev, G., Karadzhov, S., Ivanov, N., Mosin, O.V. (2015). Preparation of Electrochemically Activated Water Solutions (Catholyte/Anolyte) and Studying Their Physical-Chemical Properties. *Journal of Medicine, Physiology and Biophysics*, Vol. 16, pp. 1-14.

[Ignatov et al., 2016](#) – Ignatov, I., Gluhchev, G., Karadzhov, S., Miloshev, G., Ivanov, I., Mosin, O.V. (2015). Preparation of Electrochemically Activated Water Solutions (Catholyte/Anolyte) and Studying Their Physical-Chemical Properties. *Journal of Medicine, Physiology and Biophysics*, Vol. 11: pp. 1-21.

[Ignatov et al., 2016a](#) – Ignatov, I., Mosin, O.V., Gluhchev, G., Karadzhov, S., Miloshev, G., Ivanov, I. (2016). Studying Electrochemically Activated NaCl Solutions of Anolyte and Catholyte by Methods of Non-Equilibrium Energy Spectrum (NES) and Differential Non-Equilibrium Energy Spectrum (DNES). *Journal of Medicine, Physiology and Biophysics*, Vol. 20: pp. 13-23.

[Ignatov et al., 2016b](#) – Ignatov, I. et al. (2016). Results of Biophysical and Nano Technological Research of ZEOLITH Detox of LavaVitae Company. *Journal of Health, Medicine and Nursing*, Vol. 30, pp. 44-49.

[Ignatov, 2005](#) – Ignatov, I. (2005). Energy Biomedicine. *Gea-Libris, Sofia*, pp. 1–88.

[Ignatov, 2010](#) – Ignatov, I. (2010). Which Water is Optimal for the Origin (Generation) of Life? *Euromedica*, Hanover: 34-35.

[Ignatov, 2011](#) – Ignatov, I. (2011). Entropy and Time in Living Matter. *Euromedica*, 74 p.

[Ignatov, 2012](#) – Ignatov, I. (2012). Origin of Life and Living Matter in Hot Mineral Water, Conference on the Physics, Chemistry and Biology of Water. *Vermont Photonics*, USA.

[Ignatov, 2016](#) – Ignatov, I. (2016). Product of LavaVitae BOOST is Increasing of Energy of Hydrogen Bonds among Water Molecules in Human Body. *Journal of Medicine, Physiology and Biophysics*, Vol. 27, pp. 30-42.

[Ignatov, 2016a](#) – Ignatov, I. (2016). VITA intense – Proofs for Anti-inflammatory, Antioxidant and Inhibition Growth of Tumor Cells Effects. Relaxing Effect of Nervous System. Anti Aging Influence. *Journal of Medicine, Physiology and Biophysics*, Vol. 27, pp. 43-61.

[Ignatov, 2017](#) – Ignatov, I. (2017). Aluminosilicate Mineral Zeolite. Interaction of Water Molecules in Zeolite Table and Mountain Water Sevtopolis from Bulgaria. *Journal of Medicine, Physiology and Biophysics*, Vol. 31, pp. 41-45.

[Ignatov, 2017a](#) – Ignatov, I. (2017). VITA intense and Boost – Products with Natural Vitamins and Minerals for Health. *Journal of Medicine, Physiology and Biophysics*, Vol. 31, pp. 58-78.

[Ignatov, 2017b](#) – Ignatov, I. (2017). ZEOLITH detox for Detoxification and ZELOLITH Creme for Skin Effects as Products of LavaVitae Company. *Journal of Medicine, Physiology and Biophysics*, Vol. 31, pp. 79-86.

[Ignatov, Mosin, 2013a](#) – Ignatov I., Mosin O.V. (2013). Possible Processes for Origin of Life and Living Matter with Modeling of Physiological Processes of Bacterium *Bacillus Subtilis* in Heavy Water as Model System. *Journal of Natural Sciences Research*, Vol. 3 (9): pp. 65-76.

[Ignatov, Mosin, 2013b](#) – Ignatov, I., Mosin, O. V. (2013). Modeling of Possible Processes for Origin of Life and Living Matter in Hot Mineral and Seawater with Deuterium. *Journal of Environment and Earth Science*, Vol. 3(14), pp. 103-118.

[Ignatov, Mosin, 2013c](#) – Ignatov, I., Mosin, O. V. (2013). Structural Mathematical Models Describing Water Clusters. *Journal of Mathematical Theory and Modeling*, Vol.3 (11), pp. 72-87.

[Ignatov, Mosin, 2014a](#) – Ignatov, I., Mosin, O. V. (2014). The Structure and Composition of Carbonaceous Fullerene Containing Mineral Shungite and Microporous Crystalline Aluminosilicate Mineral Zeolite. Mathematical Model of Interaction of Shungite and Zeolite with Water Molecules. *Advances in Physics Theories and Applications*, Vol.28, pp. 10-21.

[Ignatov, Mosin, 2014b](#) – Ignatov, I., Mosin, O.V. (2014). The Structure and Composition of Shungite and Zeolite. Mathematical Model of Distribution of Hydrogen Bonds of Water Molecules in Solution of Shungite and Zeolite. *Journal of Medicine, Physiology and Biophysics*, Vol. 2, pp. 20-36.

[Ignatov, Mosin, 2014c](#) – Ignatov, I., Mosin, O.V. (2014). Mathematical Models of Distribution of Water Molecules Regarding Energies of Hydrogen Bonds. *Journal of Medicine, Physiology and Biophysics*, Vol. 2, pp. 71-94.

[Ignatov, Mosin, 2014d](#) – Ignatov, I., Mosin, O.V. (2014). Mathematical Model of Interaction of Carbonaceous Fullerene Containing Mineral Shungite and Aluminosilicate Mineral Zeolite with Water. *Journal of Medicine, Physiology and Biophysics*, Vol. 3, pp. 15-29.

[Ignatov, Mosin, 2014e](#) – Ignatov, I., Mosin, O.V. (2014). Methods for Measurements of Water Spectrum. Differential Non-equilibrium Energy Spectrum Method (DNES). *Journal of Health, Medicine and Nursing*, Vol. 6, pp. 50-72.

[Ignatov, Mosin, 2014f](#) – Ignatov, I., Mosin, O.V. (2014). Nano Mix of Shungite and Zeolite for Cleaning of Toxins and Increasing of Energy of Hydrogen Bonds among Water Molecules in Human Body. *Journal of Medicine, Physiology and Biophysics*, Vol. 27, pp. 1-10.

[Ignatov, Mosin, 2014g](#) – Ignatov, I., Mosin, O.V. (2014). Mathematical Models of Distribution of Water Molecules Regarding Energies of Hydrogen Bonds. *Journal of Medicine, Physiology and Biophysics*, Vol. 6, pp. 50-72.

[Ignatov, Mosin, 2014h](#) – Ignatov, I., Mosin, O.V. (2014). Structural Models of Water and Ice Regarding the Energy of Hydrogen Bonding. *Nanotechnology Research and Practice*, Vol. 7 (3): pp. 96-117.

[Ignatov, Mosin, 2015](#) – Ignatov, Mosin (2015). Origin of Life and Living Matter in Hot Mineral Water. *Advances in Physics Theories and Applications*, Vol. 39, 1-22.

[Ignatov, Mosin, 2016](#) – Ignatov, I., Mosin, O.V. (2016). Deuterium, Heavy Water and Origin of Life. LAP LAMBERT Academic Publishing, pp. 1-500.

[Ignatov, Mosin, 2016a](#) – Ignatov, I., Mosin, O.V. (2016). Water for Origin of Life. *Altaspera Publishing & Literary Agency Inc.* pp. 1-616. [in Russian]

[Luck et al., 1980](#) – Luck, W., Schiöberg, D., Ulrich, S. (1980). Infrared Investigation of Water Structure in Desalination Membranes. *J. Chem. Soc. Faraday Trans.*, Vol. 2(76), pp. 136-147.

[Mehandjiev et al., 2017](#) – Mehandjiev, D., Ignatov, I., Karadzhov, I., Gluhchev, G., Atanasov, A. (2017). On the Mechanism of Water Electrolysis, *Journal of Medicine, Physiology and Biophysics*, Vol. 31, pp. 23-26.

[Mosin, Ignatov, 2012](#) – Mosin, O.V., Ignatov, I. (2012). Composition and Structural Properties of Fullerene Natural Mineral Shungite. *Nanomaterials and Nanotechnologies*, 2, pp. 25-36.

[Mosin, Ignatov, 2012a](#) – Mosin, O.V., Ignatov, I. (2012). The Composition and Structural Properties of Fullerene Natural Mineral Shungite. *Nanoengineering*, Vol. 18 (12), pp. 17-24 [in Russian].

[Mosin, Ignatov, 2013b](#) – Mosin, O.V., Ignatov, I. (2013). The Structure and Composition of Natural Carbonaceous Fullerene Containing Mineral Shungite. *International Journal of Advanced Scientific and Technical Research*, Vol. 6(11–12), pp. 9–21.

[Mosin, Ignatov, 2015](#) – Mosin, O.V., Ignatov, I. (2015). An Overview of Methods and Approaches for Magnetic Treatment of Water. *Water: Hygiene and Ecology*, Vol. 3-4 (4): pp. 113-130.

[Panayotova, Velikov, 2002](#) – Panayotova, M., Velikov, B. (2002). Kinetics of Heavy Metal Ions Removal by Use of Natural Zeolite. *Journal of Environmental Science and Health*, Vol. 37(2): pp. 139–147.

[Parfen'eva, 1994](#) – Parfen'eva, L.S. (1994). Electrical Conductivity of Shungite Carbon. *Solid State Physics*, Vol. 36(1), pp. 234–236.

[Podchaynov, 2007](#) – Podchaynov, S.F. (2007). Mineral zeolite – a Multiplier of Useful Properties Shungite. Shungites and human safety. *Proceedings of the First All-Russian scientific-practical conference* (3–5 October 2006), ed. J.K Kalinin (Petrozavodsk: Karelian Research Centre of Russian Academy of Sciences), pp. 6–74 [in Russian].

Copyright © 2017 by Academic Publishing House Researcher s.r.o.



Published in the Slovak Republic  
European Journal of Medicine  
Has been issued since 2013.  
ISSN: 2308-6513  
E-ISSN: 2310-3434  
2017, 5(2): 43-55

DOI: 10.13187/ejm.2017.2.43  
[www.ejournal5.com](http://www.ejournal5.com)



## Research with Model Systems in Biophysics and Biochemistry of Bioinfluence of Dimitar Risimanski

Ignat Ignatov <sup>a, \*</sup>

<sup>a</sup> Scientific Research Center of Medical Biophysics, Sofia, Bulgaria

### Abstract

This paper presents the results of evaluation of possible biophysical methods and approaches for registering of various non-ionizing radiation (NIR) wave types of the human body in the electromagnetic and optical range. Many types of NIR (electromagnetic waves, infrared radiation, thermo radiation, bioluminescence) emitted from the human body were reviewed. In particular the results on of spontaneous biophoton emission and delayed luminescence from the human body are submitted along with *infrared thermography (IRT)* results. It was shown that 1 cm<sup>2</sup> of skin generally emits ~85 photons for 1s. The intensity of biophoton emission ranges from 10<sup>-19</sup> to 10<sup>-16</sup> W/cm<sup>2</sup> (approx. ~1–1000 photons·cm<sup>-2</sup>·s<sup>-1</sup>). The specific photon emission from part of the human thumb was detected as a spectrum of various colors with the method of Color coronal spectral analysis on a device with an electrode made of polyethylene terephthalate (PET hostafan) with applied electric voltage 15 kV, electric impulse duration 10 μs, and electric current frequency 15 kHz. It was established that photons corresponding to a red color emission of visible electromagnetic spectrum have energy at 1.82 eV. The orange color of visible electromagnetic spectrum has energy at 2.05, yellow – 2.14, blue-green (cyan) – 2.43, blue – 2.64, and violet – 3.03 eV. The reliable result measurement norm was at E ≥ 2.53 eV, while the spectral range of the emission was within 380–495 nm and 570–750 nm±5 nm. Also were estimated some important physical characteristics (energy of hydrogen bonds, wetting angle, surface tension) of water by the methods of non-equilibrium energy (NES) and differential non-equilibrium energy (DNES) spectrum of water, that helps understand in general how electromagnetic radiation interacts with water and establish the structural characteristics of water.

**Keywords:** electromagnetic waves, infrared radiation, thermo radiation, bioluminescence, color coronal spectral analysis, NES, DNES.

### 1. Introduction

All living organisms have a cellular therefore, a molecular organized structure. The living processes inside of them run on a cellular and a molecular level. Bioelectrical activity is one of the very important physical parameters of living organisms (Ignatov et al., 1998). Bioelectric potentials generated by various cells are widely used in medical diagnostics (Rubik, 2002) and are recorded as electrocardiogram, electromyogram, electroencephalogram, etc. It was proved that the human

\* Corresponding author  
E-mail addresses: [mbyoph@dir.bg](mailto:mbyoph@dir.bg) (I. Ignatov)

body and tissues emanate weak electromagnetic waves, the electric voltage of which is denoted as resting potential, action potential, omega-potential etc. (Dobrin et al., 1979; Adey, 1981). Between the outer surface of the cell membrane and the inner contents of the cell there is always the electric potential difference which is created because of different concentrations of  $K^+$ ,  $Na^+$  and  $Cl^-$  inside and outside of the cell and their different permeability through the cell membrane (Kiang et al., 2005). Their value in the human body varies  $\sim 50\text{--}80$  mV and is defined by the galvanic contact of a voltmeter input with an object that indicates on the galvanic type of their source (Cleary, 1993). When being excited a living cell changes the membrane electric potential due to changes in membrane permeability and active ion movement through the membrane. In cells of excitable tissues (muscle, nervous), these processes can occur within a very short time intervals (milliseconds) and are called “current action” potential. Its magnitude makes up  $\sim 120$  mV. Electromagnetic fields refer to non-ionizing radiation (NIR), i.g. the radiative energy that, instead of producing charged ions when passing through matter, has sufficient energy only for excitation. Nevertheless it is known to cause biological effects (Kwan-Hoong, 2003). The NIR spectrum is divided into two main regions, optical radiations and electromagnetic fields. The optical spectrum can be further sub-divided into ultraviolet, visible, and infra-red. The electromagnetic fields are further divided into radiofrequency (microwave, very high frequency and low frequency radio wave). NIR encompass the long wavelength ( $> 100$  nm) and low photon energy ( $< 12.4$  eV) portion of the electromagnetic spectrum, from 1 Hz to  $3 \cdot 10^{15}$  Hz. As a result of research carried out in the 1990-s and subsequent years, it was established the property of animal and plant tissues to generate relatively strong transient NIR electric fields due to mechanical stresses and temperature changes in biological structure (Anderson, 1993). These electric fields are mainly due to the piezoelectric and pyroelectric voltage electric polarization of natural biological structures. Owing to cell metabolism, electric dipoles (polar and ionized molecules) involved in polarization of biostructures are continuously destroyed and restored, i.e. this is a non-equilibrium polarization (Barnes, Greenebaum, 2006). Such type of non-equilibrium electric polarization is known as a main characteristic of electrets (Gubkin, 1978). Electrets include dielectric insulators and semiconductors, which under certain conditions, i.g. under the influence of a strong electrostatic field or ionizing radiation, light and other factors acquire property to generate an external electric field, existing for a long time (days, years) and slowly diminishes because the destruction of their substance by polarization (Sessler, Gerhard-Multhaupt, 1998). Along with the electromagnetic field electrets generate specific electric currents produced by heating – thermally stimulated current (TSC) (Gross, 1964). Electrets belong to the non-galvanic type of electrical sources, which tend to a strong electric field (up to  $10^6$  V/m) and the infinitesimal electric current ( $\sim 10^{-14}$  A/mm<sup>2</sup>). By analogy with the physical fields the electric field emitted from the human body on its physical characteristics resembles the electric field generated by electrets. The electrets play an important role in functioning of many biological structures as they themselves possess electret properties. The bioelectret field registered on the surface of the human body basically are generated by the basal cells of the epidermis (Marino, 1988). Dermis cells adjacent to the bottom layer of basal cells are surrounded by a conductive interstitial fluid, which electric voltage while grounding of the human body is close to zero (so called ground potential). This interstitial fluid screens off electromagnetic fields of underlying tissues. With the average thickness of the epidermis ( $\sim 0.1$  mm) and the maximum value of electric voltage ( $\sim 30.0$  V), the electric field strength can reach significant values at  $\sim 300000$  V/m (Seto et al., 1992). The strength of the electric field is quiet sufficient for its influence on the biological processes in cells and surrounding tissues, including the synthesis of proteins and nucleic acids (Liboff et al., 1984; Frey, 1993; Shimizu et al., 1995). This electric field along with the field of transmembrane assymetry of ions concentrated at inside and outside of the membrane ( $\sim 10^5$  V/cm<sup>2</sup>) can participate in the cooperative effects in cell membrane structures (Holzel, Lamprecht, 1994; Miller, 1986). Thus, owing to the bioelectret condition of certain subcellular structures in the cell and its surroundings is generated slowly oscillating electric field that is strong enough to influence the biological processes. This field and the electric field due to the piezoelectric voltage and intramembrane electric field forms the total electromagnetic field of the cell and its supracellular structures. It is known that the human skin emanates electromagnetic waves in close ultraviolet range, optic range and also in close infrared range. Infrared thermal bioradiation is found in the middle infrared range at wavelengths from 8 to 14  $\mu\text{m}$ . At wavelength



of 9.7  $\mu\text{m}$  infrared bioradiation has its maximum value at  $t = 36.6$  °C. At this temperature the skin emission is closest to the emission of absolute black body (ABB) being at the same temperature. Infrared emission penetrates the skin surface at a depth of  $\sim 0.1$  mm, and is reflected in accordance with the physical laws of reflection of the visible part of the electromagnetic spectrum. Evidently, radiation energy influences tissues while being absorbed by them. Yu.V. Gulyaev and E.E. Godik (Gulyaev, Godik, 1984) determined that the threshold of skin sensitivity for infrared radiation compiled  $\sim 10^{-14}$  W/cm<sup>2</sup>. When thermal influence is applied to the point of threshold skin sensitivity, there is developed a physiological reaction toward the thermal current. The intensity of the radiated thermal current generated by skin makes up  $\sim 2.6 \cdot 10^{-2}$  W/cm<sup>2</sup>. The second component of electromagnetic waves is bioluminescence (Young, Roper, 1976; Chang et al., 1998). It is supposed that biophotons, or ultraweak photon emissions of biological objects, are weak electromagnetic waves in the optical range of the spectrum (Cohen, Popp, 1997). The typical observed emission of biological tissues in the visible and ultraviolet frequencies ranges from  $10^{-19}$  to  $10^{-16}$  W/cm<sup>2</sup> ( $\sim 1$ – $1000$  photons $\cdot\text{cm}^{-2}\cdot\text{sec}^{-1}$ ) (Edwards et al., 1989; Choi et al., 2002). This light intensity is much weaker than that one to be seen in the perceptually visible and well-studied spectrum of normal bioluminescence detectable above the background of thermal radiation emitted by tissues at their normal temperature (Niggli, 1993). Bioelectric emission from parts of the human body as thumbs can be easily detected with the method of Color coronal spectral analysis under applying gas electrical discharge of high voltage and frequency developed by I. Ignatov (Ignatov, 2005). This method has big scientific and practical prospects in biophysics and medical diagnostics (Chiang et al., 2005). Its advantages include safety, sterility, clarity and interpretability of the data obtained, ease of storage and subsequent computer data processing, the ability to monitor the development of processes in time, comparing the structural, functional and temporal processes etc. The purpose of this research was studying of possible biophysical methods and approaches for registering various NIR wave's types emitted from the human body (electromagnetic waves, infrared radiation, thermo radiation) and methods of their visualization by different technique including magnetography, *infrared thermography*, *chemiluminescence*, and color coronal gas discharge spectral analysis.

## 2. Materials and Methods

### 2.1. Registration of electromagnetic fields

The registration of electromagnetic fields was used with super conductive detectors based on Josephson junctions – device made by sandwiching a thin layer of insulating nonsuperconducting material between two layers of superconducting cooper pairs (S-I-S). This allows the registering of magnetic fields  $10^{10}$  times weaker than the Earth's magnetic field. The study of electric field nearby the human body was done using a standard Faraday cage formed by conducting material (aluminium foil) blocks external static and non-static electric fields by channeling electricity through the conducting material, providing constant voltage on all sides of the enclosure.

### 2.2. Color coronal gas discharge spectral analysis

Experiments were carried out by using selective high-frequency electric discharge (SHFED) on a device with the electrode made of polyethylene terephthalate (PET, hostafan) with an electric voltage on the electrode 15 kV, electric impulse duration 10  $\mu\text{s}$ , and electric current frequency 15 kHz. The electrode of the device was made of hostafan, and was filled up with electro-conductive fluid. The spectral range of the emission was in the range 380–495 nm and 570–750 $\pm$ 5 nm. The measurements were measured in electronvolts (eV). Detection of gas discharge glowing was conducted in a dark room equipped with a red filter. On the electrode put a photosensitive paper or color film. The object under study (human thumb) was placed on top of a sheet of photo paper or color film. Between the object and the electrode were generated impulses of the electric voltage 15 kV and electric current frequency – 15–24 kHz; on the reverse side of the electrode was applied the transparent electrically conductive thin copper coating. Under these conditions in the thin contact gas space between the studied object and electrode was generated gas electric discharge in the form of characteristic glow around the object – a corona gas electric discharge in the range of 280–760 nm, illuminates a color photo or a photographic film on which was judged about the bioelectric properties of the studied object. Along with the visible range, for this method were obtained color spectra in UV and IR range. Evaluation of the characteristic parameters of

snapshots was based on the analysis of images treated by standard software package. Statistical processing of the experimental data was performed using the statistical package STATISTISA 6 using Student's t-criterion (at  $p < 0.05$ ).

### 2.3. NES and DNES experiments on interaction of electromagnetic field with water

The research was made with the method of non-equilibrium spectrum (NES) and differential non-equilibrium spectrum (DNES). The device measures the angle of evaporation of water drops from  $72^\circ$  to  $0^\circ$ . As the main estimation criterion was used the average energy ( $\Delta E_{H...O}$ ) of hydrogen O...H-bonds between  $H_2O$  molecules in water's samples. The spectrum of water was measured in the range of energy of hydrogen bonds  $0.08-0.1387$  eV or  $8.9-13.8$   $\mu m$  with using a specially designed computer program. The study with Risimanski was performed with deionized water and 1 % of glucose solution.

## 3. Results and Discussion

### 3.1. Color coronal gas discharge spectral analysis

Coronal gas discharge effect is indicated by the glow corona electrical discharge (flooding, crown, streamer) on the surface of objects being placed in the alternating electric field of high frequency (10–150 kHz) and electric voltage (5–30 kV) (Kilrian, 1949). In this process in the ionization zone develops the gas corona discharge sliding on dielectric surface, occurring in a nonuniform electric field near the electrode with a small radius of curvature. In the thin air layer with thickness of  $\sim 10-100$   $\mu m$  between the studied object and the electrode are developed the following processes:

1) Excitation, polarization and ionization by electric field of high frequency the main components of air – the molecules of nitrogen (78 %  $N_2$ ), oxygen (21 %  $O_2$ ) and carbon dioxide (0.046 %  $CO_2$ ). In the result of this is formed an ionized gas, i.e. gas with separated electrons having negative charges, creating a conductive medium as plasma;

2) Formation of a weak electric current in the form of free electrons separated from molecules of  $N_2$ ,  $O_2$  and  $CO_2$ , which generate gas discharge between the studied object and the electrode. The form of gas discharge glowing, its density and surface brightness distribution is determined mainly by electromagnetic properties of the object;

3) The transition of electrons from lower to higher energy levels and back again, during which there appears a discrete quantum of light radiation in the form of photon radiation. The transition energy of electrons depends on the external electric field and the electronic state of the studied object. Therefore, in different areas surrounding the electric field, the electrons receive different energy impulses, i.e. “skipping” at different energy levels those results in emission of photons with different wavelengths (frequencies) and the energy, coloring the contour of the glow in various spectral colors. Processes outlined above form the total gas electric effect (Ignatov, Mosin, 2012), allows to study the electrical properties of the object at its interaction with an external electromagnetic field (Ignatov, Mosin, 2013a; Ignatov, Mosin, 2013b). It was shown that the electrical conductivity of the object has almost no effect on the formation of the electric images, which mostly depends on the dielectric constant (Pehek et al., 1976).

There is a relationship (1) of the electric discharge per unit area of the recording medium on the following parameters:

$$\sigma = [\alpha - U_p(d_2 + \delta)/d_2] \epsilon_0(d_2 + \delta) / \delta d_2, \quad (1)$$

$$\text{where: } \delta = d_1/\epsilon_1 + d_3/\epsilon_3$$

$\alpha$  – slope rate of electrical pulse;

T – duration of the electrical pulse;

$U_p$  – breakdown voltage of the air layer between the subject and the recording medium;

$d_1$  – the width of the object;

$d_2$  – width of the zone of influence of the electromagnetic field;

$d_3$  – width of the recording medium;

$\epsilon_0$  – dielectric permittivity of the air ( $\epsilon_0 = 1.00057$  F/m);

$\epsilon_1$  – dielectric permittivity of the studied object;

$\epsilon_3$  – dielectric permittivity of the medium.

To calculate the breakdown voltage of the air layer is used this formula:

$$U_p = 312 + 6,2d_2 \quad (2)$$

As a result of mathematical transformations is obtained a quadratic equation describing the width of the air layer:

$$6,2d_2^2 - (\alpha T - 6,2\delta - 312)d_2 + 312\delta = 0 \quad (3)$$

This equation has two solutions:

$$d_2 = [\alpha T - 6,2\delta - 312] \pm [(\alpha T - 6,2\delta - 312)^2 - 7738\delta]^{1/2} \quad (4)$$

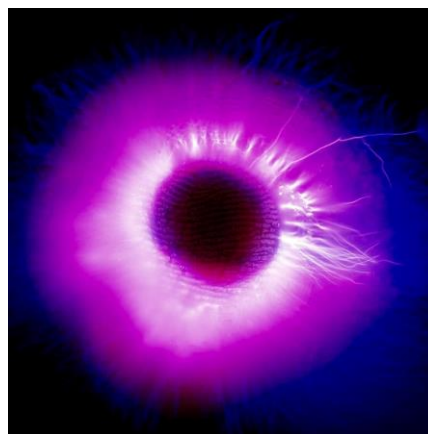
The above equations allow calculating maximum and minimum width of the air layer for the occurrence of electric discharge under which is being formed the electrical image of the studied object. Gas discharge characteristics for various biological objects vary in character and light intensity, size of contour glow and color spectrum and depend both on its own electromagnetic radiation and the dielectric constant of the object. The intensity depends on the electric voltage applied on the electrode. Studies have shown that the contours of gas discharge glow at 12 kHz and 15 kHz are homogeneous in their structure. The contour at kHz is 55 % of the contour at 15 kHz and at 24 kHz – only 15 % of the contour at 15 kHz that is important for further analysis and identification of images. The incidence of bioelectrical activity of the body reducing the intensity of gas discharge glow. Pathology in the organism and surrounding tissues also alter the bioelectric activity and the shape and color of gas discharge glow, which is determined mainly by energy of photon emission at the transition of electrons from higher energy levels to the lower ones when being excited by the external electric field. Thus, for red color of the electromagnetic spectrum this energy compiles 1.82 eV, for orange color – 2.05 eV, yellow – 2.14 eV, blue-green (cyan) – 2.43 eV, blue – 2.64 eV, and violet – 3.03 eV. The reliable result norm is at  $E \geq 2.53$  eV.

The spectral range of the photon emission for different colors is within 380-495 nm and 570–750 nm±5 nm. The photons, corresponding to the emission with green color in the visible electromagnetic spectrum, are not being detected under those experimental conditions. Thus, the more predominant in the color spectrum yellow, orange, blue, blue-green and purple colors, the more pronounced is gas discharge glow and bioelectric properties of the object. According to the data obtained, the incidence of bioelectrical activity of the body reducing the intensity of gas discharge glow. Studies carried out by A. Antonov and I. Ignatov on 1120 patients shown that the overall drop in the bioelectric activity of the body, as well as pathology in organism alter the bioelectric activity and reduce the apparent size of the gas discharge glow. This dependence is observed for many disorders, although there are not statistical reliable results that this method can be applied in medical diagnostics. The research area was from part of the thumb contacted with transparent electrode. The norm of energy of photon emission compiles 2.54 eV. If the value is over than 2.54 eV this is an indicator of normal bioelectrical status. Some people with high energy status possess the values of photon emission over 2.90 eV. The high values of this parameter are possible with practicing of yoga, sport etc. The emission less than 2.53 eV is characteristic for people with low bioelectrical status. These results are interesting from scientific point of view, because they may provide brilliant prospects for further using of this method for biophysical studies. interesting from scientific point of view, because they may provide prospects for further using of this method for biophysical studies.

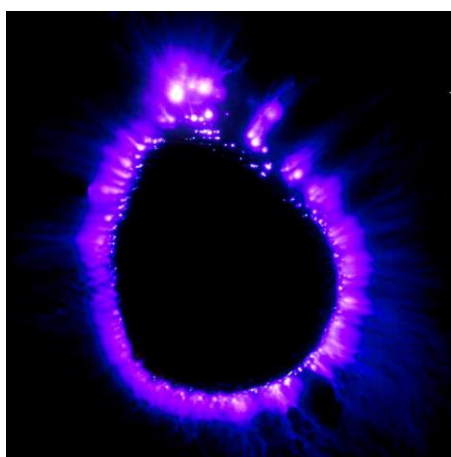
Figure 1 shows the results of of Dimitar Risimanski with color coronal discharge. The bioelectrical discharge in norm is on fig. 1a). The code of bioelectrical photography of Risimanski is 1b). The coronal image of the man A.A. before bioinfluence of Risimanski is 3c). The picture is with blue biophoton emission 2.64 eV. The result of the man A.A. after influence on Risimanski is 3d). It is with biophoton emission with blue and predominant violet color and biophoton emission – 3.00 eV.



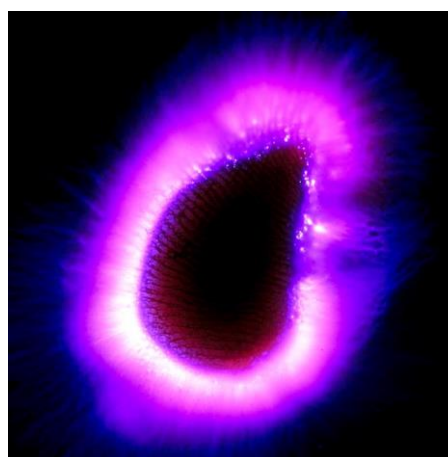
a). Bioelectrical discharge of a person in norm (1.94 eV)



b). Bioelectrical discharge image of Dimitar Risimanski (3.03 eV)



c). Bioelectrical discharge image of A.A.. (2.64 eV)



d). Bioelectrical discharge image of A.A. (3.00 eV)

**Fig. 1.** Bioelectrical discharge images of the research with Dimitar Risimanski (I. Ignatov)

### 3.2. NES and DNES analysis of water

Water seems to be a good model system for studying the interaction with electromagnetic field and structural research. The recent data indicated that water is a complex associated non-equilibrium liquid consisting of associative groups (clusters) containing from 3 to 50 individual H<sub>2</sub>O molecules (Keutsch, Saykally, 2011). These associates can be described as unstable groups (dimers, trimers, tetramers, pentamers, hexamers etc.) in which individual H<sub>2</sub>O molecules are linked by van der Waals forces, dipole-dipole and other charge-transfer interactions, including hydrogen bonding (Ignatov, Mosin, 2013c). At room temperature, the degree of association of H<sub>2</sub>O molecules may vary from 2 to 21. The measurements were performed with using NES and DNES methods. It was established experimentally that the process of evaporation of water drops, the wetting angle  $\theta$  decreases discretely to 0, and the diameter of water drop basis is only slightly altered, that is a new physical effect (Antonov, Yuskesslieva, 1983). Based on this effect, by means of measurement of the wetting angle within equal intervals of time is determined the function of distribution of H<sub>2</sub>O molecules according to the value of  $f(\theta)$ . The distribution function is denoted as the energy spectrum of the water state. A theoretical research established the dependence between the surface tension of water and the energy of hydrogen bonds among individual H<sub>2</sub>O-molecules (Antonov, 1995). The hydrogen bonding results from interaction between electron-deficient H-atom of one H<sub>2</sub>O molecule (hydrogen donor) and unshared electron pair of an electronegative O-atom (hydrogen acceptor) on the neighboring H<sub>2</sub>O molecule; the structure of hydrogen bonding may be defined as  $O \cdots H^{\square+} - O^{\square}$ .

For calculation of the function  $f(E)$  represented the energy spectrum of water, the experimental dependence between the wetting angle ( $\theta$ ) and the energy of hydrogen bonds ( $E$ ) is established:

$$f(E) = b \times f(\theta) / 1 - (1 + b \times E)^{1/2}, \quad (4)$$

$$\text{where } b = 14.33 \text{ eV}^{-1} \quad (5)$$

The relation between the wetting angle ( $\theta$ ) and the energy ( $E$ ) of the hydrogen bonds between  $H_2O$  molecules is calculated by the formula:

$$\theta = \arcsin(-1 - 14.33E) \quad (6)$$

The energy spectrum of water is characterized by a non-equilibrium process of water droplets evaporation, therefore, the term non-equilibrium spectrum (NES) of water is used. The energy of hydrogen bonds measured by NES is determined as  $\bar{E} = -0,1067 \pm 0,0011 \text{ eV}$ .

The difference  $\Delta f(E) = f(\text{samples of water}) - f(\text{control sample of water})$  – is called the “differential non-equilibrium energy spectrum of water” (DNES).

Thus, DNES spectrum is an indicator of structural changes of water as a result of various external factors. The cumulative effect of these factors is not the same for the control sample of water and the water sample being under the influence of this factor.

Figure 2 shows NES-spectrum of deionized water that was used as a model system for studying the interaction of electromagnetic field with water. On the X-axis are given three scales. The energies of hydrogen bonds among  $H_2O$  molecules are calculated in eV. On the Y-axis is shown the energy distribution function  $f(E)$  of  $H_2O$  molecules measured in  $eV^{-1}$ . It was shown that the window of transparency of the earth atmosphere for the electromagnetic radiation in the middle IR-range almost covers NES-spectrum of water. Arrows A and B designate the energy of hydrogen bonds among  $H_2O$  molecules. Arrow C designates the energy at which the human body behaves itself as absolute black body (ABB) at optimum temperature  $36.6 \text{ }^\circ\text{C}$  and adsorbs the thermal radiation. A horizontal arrow designates the window of transparency of the earth atmosphere for the electromagnetic radiation in the middle IR-range.

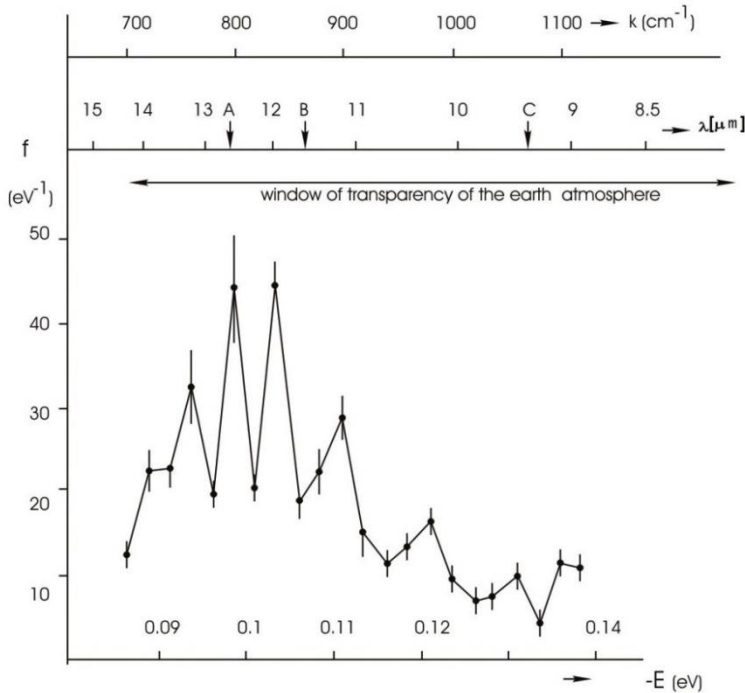


**Fig. 2.** Non-equilibrium energy spectrum (NES) of water as a result of measurement for 1 year:  $\lambda$  – wavelength,  $k$  – wave number

Another important physical parameter was calculated with using NES and DNES methods – the average energy ( $\Delta E_{H...O}$ ) of H...O-bonds between H<sub>2</sub>O compiled  $-0.1067 \pm 0.0011$  eV. The most remarkable peculiarity of H...O-bond consists in its relatively low strength; it is 5–10 times weaker than chemical covalent bond. In respect of energy hydrogen bond has an intermediate position between covalent bonds and intermolecular van der Waals forces, based on dipole-dipole interactions, holding the neutral molecules together in gasses or liquefied or solidified gasses. Hydrogen bonding produces interatomic distances shorter than the sum of van der Waals radii, and usually involves a limited number of interaction partners. These characteristics become more substantial when acceptors bind H atoms from more electronegative donors. Hydrogen bonds hold H<sub>2</sub>O molecules on 15 % closer than if water was a simple liquid with van der Waals interactions. The hydrogen bond energy compiles 5–10 kcal/mole, while the energy of covalent O–H-bonds in H<sub>2</sub>O molecule – 109 kcal/mole. With fluctuations of water temperature the average energy of hydrogen H...O-bonds in H<sub>2</sub>O molecule associates changes. That is why hydrogen bonds in liquid state are relatively weak and unstable: it is thought that they can easily form and disappear as the result of temperature fluctuations. The next conclusion that can be drawn from our research is that there is the distribution of energies among individual H<sub>2</sub>O molecules.

Further we performed two types of temperature-dependent experiments on heat exchange from the surface of the human body by DNES-method. In first experiment we studied heat exchange when the temperature of the human body was higher than the temperature of the surrounding environment (curve 1a and 1b on Fig. 3). In second experiment there was heat exchange when the temperature of the human body was lower than that of the surrounding environment (curve 2a and 2b on Fig. 3). In both experiments it was detected a local maximum at  $9.7 \mu\text{m}$  on curve 1 and curve 2 (Fig. 3). This local maximum corresponds to the maximal level of heat emission from the surface of the human body and lays within the “transparency window” of Earth atmosphere to electromagnetic radiation in the mid IR-range of the electromagnetic spectrum. In this range, the electromagnetic radiation emitted by the earth in the surrounding space is being absorbed by the Earth atmosphere. There is a statistical difference between the results of heat emission from the surface of the human body to the surrounding environment and back to the human body according to the *t*-criterion of Student at  $p < 0.01$ . The local maximum on curve 1a is detected at  $7.3 \text{ eV}^{-1}$ , while the local maximum on curve 2a – at  $2.4 \text{ eV}^{-1}$  (Fig. 3). The result of Dimitar Risimanski from him to environment is  $(-7.2 \text{ meV})$ . The result of Dimitar Risimanski from environment to him is  $(7.1 \text{ meV})$ . The difference is definite as effective energy is  $(-7.5) - (7.5) = (-15.0) \text{ meV}$ .

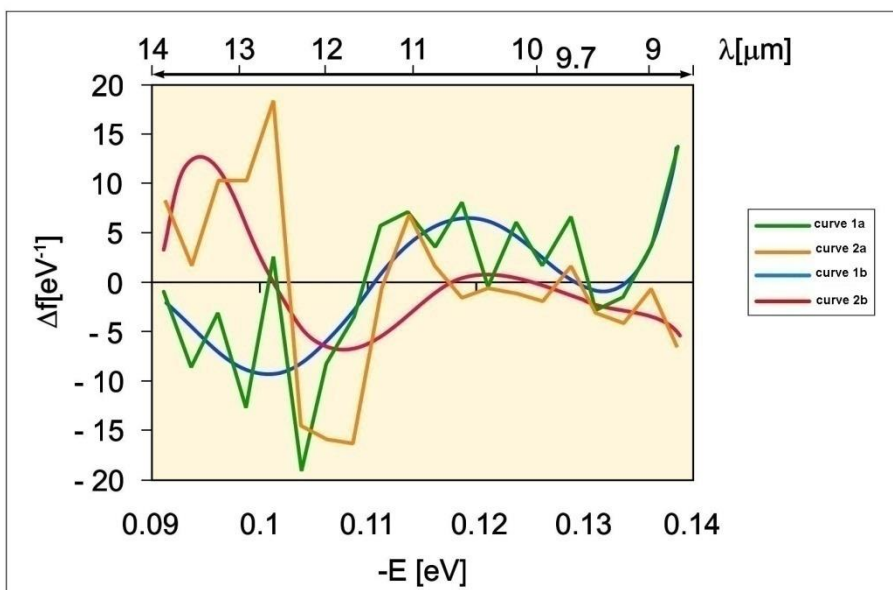


**Fig. 3.** Differential non-equilibrium energy spectrum (DNES) reflecting the heat exchange of the human body with surrounding environment

#### 4. Conclusion

In frames of this research many types of NIR radiation (electromagnetic waves, infrared radiation, thermo radiation, and bioluminescence) emitted from the human body were studied and carefully scrutinized. The approaches and methods for detecting various types of radiation employed in this research as magnetography, chemiluminescence and color coronal gas discharge spectral analysis can find further application in many branches of applied science and medical diagnostics, while other methods as NES and DNES may be applied for studying the interaction of electromagnetic fields with water and structural studies. The research of Risimanski's bioinfluence was performed with two model systems. First is biophysical analysis on water spectrum. Second is biochemical analysis with 1 % solution of glucose. In the report are presented the phenomenal biophysical results of influence of Dimitar Risimanski (Bulgaria). The results are base for additional biochemical, biological and medical research projects.

#### References

- Adey, 1981 – Adey, W.R. (1981). Tissue Interaction with Non-ionizing Electromagnetic Fields. *Physiol. Rev.*, 61, pp. 435–514.
- Anderson, 1993 – Anderson, L.E. (1993). Biological Effect of Extremely Low Frequency Electromagnetic Fields: in Vivo Studies. *Am. Ind. Hyg. Assoc. J.*, 54, pp. 186–196.
- Anosov, Trukhan, 2003 – Anosov V.N., Trukhan E.M. (2003). A New Approach to the Problem of Weak Magnetic Fields: An Effect on Living Objects. *Doklady Biochemistry and Biophysics*, 392 (1-6): 274-278.
- Antonov, 1995 – Antonov, A. (1995). Research of the Non-equilibrium Processes in the Area in Allocated Systems. Dissertation thesis “Doctor of physical sciences”, Blagoevgrad, Sofia.
- Antonov, Yuskesseliyeva, 1985 – Antonov, A., Yuskesseliyeva, L. (1985). Selective High Frequency Discharge (Kirlian effect). *Acta Hydrophysica*, Berlin, 5, 29 p.
- Barnes, Greenebaum, 2006 – Barnes, F.S., Greenebaum, B. (eds.) (2006). CRC Handbook on Biological Effects of Electromagnetic Fields. 3d Edition. Boca Raton: CRC Press, Vol. 2, 960 p.
- Bars, Andre, 1976 – Bars, Le., Andre, G. (1976). Biological Effects of Electric Fields on Rats and Rabbits. *Red. Gen. Elect.* (special issue), pp. 91–97.
- Belousov et al., 1997 – Belousov, L.V., Opitz, J.M., Gilbert, S.F. (1997). Life of Alexander G. Gurwitsch and His Relevant Contribution to the Theory of Morphogenetic Fields. *The International journal of developmental biology*, 41(6): pp. 7–771.
- Belousov et al., 2000 – Belousov, L., Popp, F.A., Voeikov, V., van Wijk, R. (eds) (2000). Biophotonics and Coherent Systems. *Moscow University Press*, 133 p.
- Boveris et al., 1980 – Boveris, A., Cadenas, E., Reiter, R., Filipkowski, M., Nakase, Y., Chance, B. (1980). Organ chemiluminescence: Noninvasive assay for oxidative radical reactions. *Proc. Natl. Acad. Sci. USA*, Vol. 77, pp. 347–351.
- Chang et al., 1998 – Chang, J.J., Fisch, J. & Popp, F.A. (eds) (1998). Biophotons. Dordrecht. *Kluwer Academic Publishers*, 417 p.
- Chiang et al., 2005 – Chiang, L.H, Wah Khong, P. & Ghista, D. (2005). Bioenergy Based Medical Diagnostic Application Based on Gas Discharge Visualization. *Conf Proc IEEE Eng. Med. Biol. Soc.*, Vol. 2, 1533 p.
- Choi et al., 2002 – Choi, C., Woo, W.M., Lee, M.B. at al. (2002). Biophoton Emission From the Hands. *J. Korean Physical. Soc.*, Vol. 41, pp. 275–278.
- Cleary, 1993 – Cleary, S.F. (1993). A Review of in Vitro Studies: Low-frequency Electromagnetic Fields. *J. Am. Ind. Hyg. Assoc.*, Vol. 54(4), pp. 178–185.
- Cohen, 1968 – Cohen, D. (1968). Magnetoencephalography: Evidence of Magnetic Fields Produced by Alpha-rhythm Currents. *Science*, Vol. 161(3843), pp. 784–786.
- Cohen, Popp, 1997 – Cohen, S., Popp, F.A. (1997). Biophoton emission of the human body. *Journal of Photochemistry and Photobiology B: Biology*, 40(2): 187–189.
- Devaraj et al., 1997 – Devaraj, B., Usa, M., Inaba, H. (1997). Biophotons: Ultraweak Light Emission from Living Systems. *Curr. Opin. Solid State Mater Sci.*, Vol. 2, 188.
- Dobrin et al., 1979 – Dobrin, R., Kirsch, C., Kirsch, S. et al. (1979). Experimental Measurements of the Human Energy Field. In S. Krippner (ed.). *Psychoenergetic Systems: The Interface of Consciousness, Energy and Matter*. New York, Gordon & Breach, 230 p.

Esterbauer et al., 1990 – Esterbauer, H., Zollner, H., Schaur, R. J. (1990). Aldehydes Formed by Lipid Peroxidation: Mechanisms of Formation, Occurrence, and Determination. In Membrane Lipid Oxidation. Boca Raton, CRC Press, 283 p.

Frey, 1993 – Frey, A.H. (1993). Electromagnetic Field Interactions with Biological Systems. *FASEB Journal*, Vol. 7(2): pp. 272–281.

Gerardi et al., 2008 – Gerardi, G., De Ninno A., Prosdocimi, M. et al. (2008). Effects of Electromagnetic Fields of Low Frequency and Low Intensity on Rat Metabolism. *Biomagnetic Research and Technology*, 6: 3.

Goodman et al., 1995 – Goodman, R., Greenbaum, B. & Marron, M.T. (1995). Effects of Electromagnetic Fields on Molecules and Cells. *Int. Rev. Cytol.*, 158: 279–338.

Gross, 1964 – Gross, B. (1964). Charge Storage in Solid Dielectrics; a Bibliographical Review on the Electret and Related Effects. New York, Elsevier Pub. Co., 230.

Gubkin, 1978 – Gubkin, A.N. (1978). Electrets. Moscow, Nauka. 192 p.

Gulyaev, Godik, 1984 – Gulyaev, Yu.V., Godik, E.E. (1984). On the Possibilities of the Functional Diagnostics of the Biological Subjects Via Their Temporal Dynamics of the Infrared Images. *USSR Academy Nauk Proceedings/Biophysics*, Vol. 277, pp. 1486–1491.

Gulyaev, Godik, 1990 – Gulyaev, Yu.V., Godik, E.E. (1990). Human and Animal Physical Fields. // *Scientific American*, Vol. 5, pp. 74–83.

Gulyaev, Godik, 1991 – Gulyaev, Yu.V., Godik, E.E. (1991). Functional Imaging of the Human Body. *IEEE Engineering in Medicine and Biology*, Vol. 10, pp. 21–29.

Gurwitsch, 1959 – Gurwitsch, A.G. (1959). Die Mitogenetische Strahlung, Ihre Physikalisch-chemischen Grundlagen und Ihre Anwendung in Biologie und Medizin. Jena, Germany, Veb G. Fisher.

Gurwitsch, 1988 – Gurwitsch, A.G. (1988). A historical Review of the Problem of Mitogenetic Radiation. *Experientia*, Vol. 44: 545–550.

Halliwell, Gutteridge, 1989 – Halliwell, B., Gutteridge, J.M.C. (1989). Free Radicals in Biology and Medicine (2nd ed.). Oxford, Clarendon Press.

Hastings, 1983 – Hastings, J.W. (1983). Biological Diversity, Chemical Mechanisms, and the Evolutionary Origins of Bioluminescent Systems. *J. Mol. Evol.*, 19(5): 309–321.

Holzel, Lamprecht, 1994 – Holzel, R., Lamprecht, I. (1994). Wirkungen Elektromagnetischer Felder auf biologische Systeme. *Nachrichtentech Elektron.* Vol. 44(2), pp. 28–32.

Ignatov et al., 1998 – Ignatov, I., Antonov, A., Galabova, T. (1998). Medical Biophysics – Biophysical Fields of Man. *Gea Libris, Sofia*, pp. 1–71.

Ignatov et al., 2002 – Ignatov, I., Antonov, A., Galabova, T. (2002). Scientific Research Studies with Christos Drossinakis (October 2001 – October 2002). *Int. Conference “Man and Nature”*, SRCMB, Sofia.

Ignatov et al., 2014 – Ignatov, I., Mosin, O. V., Stoyanov, Ch. (2014). Fields in Electromagnetic Spectrum Emitted from Human Body. Application in Medicine. *Journal of Health, Medicine and Nursing*, Vol. 7, pp. 1-22.

Ignatov et al., 2014a – Ignatov, I., Mosin, O. V., Niggli, H., Drossinakis, Ch. (2014). Evaluating of Possible Methods and Approaches for Registering of Electromagnetic Waves Emitted from the Human Body. *Advances in Physics Theories and Applications*, Vol. 30, pp. 15-33

Ignatov et al., 2014b – Ignatov, I., Mosin, O.V., Drossinakis, Ch. (2014). Infrared Thermal Field Emitted from Human Body. Thermovision. *Journal of Medicine, Physiology, Biophysics*, Vol.1, pp. 1-12.

Ignatov et al., 2014c – Ignatov, I., Mosin, O. V., Niggli, H., Drossinakis, Ch., Stoyanov, Ch. (2014). Registration of Electromagnetic Waves Emitted the Human Body. *Journal of Medicine, Physiology and Biophysics*, Vol. 5, pp. 1-22.

Ignatov et al., 2014d – Ignatov, I., Mosin, O. V., Niggli, H., Drossinakis, Ch. (2014). Evaluating of Possible Methods and Approaches for Registering Electromagnetic Waves Emitted from the Human Body. *Nanotechnology Research and Practice*, Vol. 2 (2), pp. 96-116.

Ignatov et al., 2014e – Ignatov, I., Mosin, O.V., Stoyanov, Ch. (2014). Biophysical Fields. Color Coronal Spectral Analysis. Registration with Water Spectral Analysis. Biophoton Emission. *Journal of Medicine, Physiology and Biophysics*, Vol. 6, pp. 1-22.



[Ignatov et al., 2015](#) – Ignatov, I., Mosin, O.V., Niggli, H., Drossinakis, Ch. (2015). Evaluation of Possible Methods and Approaches for Registering Non-Ionizing Radiation (NIR) Waves Emitting from the Human Body. *Journal of Pharmacy and Alternative Medicine*, Vol. 4, pp. 57-75.

[Ignatov et al., 2016](#) – Ignatov, I. et al. (2016). Results of Biophysical and Nano Technological Research of ZEOLITH Detox of LavaVitae Company. *Journal of Health, Medicine and Nursing*, Vol. 30, pp. 44-49.

[Ignatov, 2005](#) – Ignatov, I. (2005). Energy Biomedicine. *Gea-Libris, Sofia*: pp. 1–88.

[Ignatov, 2016a](#) – Ignatov, I. (2016). Product of LavaVitae BOOST is Increasing of Energy of Hydrogen Bonds among Water Molecules in Human Body. *Journal of Medicine, Physiology and Biophysics*, Vol. 27., pp. 30-42.

[Ignatov, 2016b](#) – Ignatov, I. (2016). VITA intense – Proofs for Anti-inflammatory, Antioxidant and Inhibition Growth of Tumor Cells Effects. Relaxing Effect of Nervous System. Anti Aging Influence. *Journal of Medicine, Physiology and Biophysics*, Vol. 27. pp. 43-61.

[Ignatov, 2017](#) – Ignatov, I. (2017). Aluminosilicate Mineral Zeolite. Interaction of Water Molecules in Zeolite Table and Mountain Water Sevtopolis from Bulgaria. *Journal of Medicine, Physiology and Biophysics*, Vol. 31, pp. 41-45.

[Ignatov, 2017a](#) – Ignatov, I. (2017). VITA intense and Boost – Products with Natural Vitamins and Minerals for Health. *Journal of Medicine, Physiology and Biophysics*, Vol. 31, pp. 58-78.

[Ignatov, 2017b](#) – Ignatov, I. (2017). ZEOLITH detox for Detoxification and ZEOLITH Creme for Skin Effects as Products of LavaVitae Company. *Journal of Medicine, Physiology and Biophysics*, Vol. 31, pp. 79-86.

[Ignatov, Mosin, 2014](#) – Ignatov, I., Mosin, O. V. (2014). Coronal Gas Discharge Effect in Modeling of Non-Equilibrium Conditions with Gas Electric Discharge Simulating Primary Atmosphere and Hydrosphere for Origin of Life and Living Matter, *Journal of Medicine, Physiology and Biophysics*, 5: 47-70.

[Ignatov, Mosin, 2012](#) – Ignatov, I., Mosin, O.V. (2012). Coronal Effect in Biomedical Diagnostics and Study of Bioenergetical Properties of Biological Objects and Water. *Biomedical Radio electronics, Biomedical Technologies and Radio Electronics*, Vol. 12, pp. 13–21 [in Russian].

[Ignatov, Mosin, 2013a](#) – Ignatov, I., Mosin, O.V. (2013). Method for Color coronal (Kirlian) Spectral Analysis. *Biomedical Radio electronics, Biomedical Technologies and Radio Electronics*: Vol. 1, pp. 38–47 [in Russian].

[Ignatov, Mosin, 2013b](#) – Ignatov, I., Mosin O.V. (2013b). Color Crown Spectral Kirlian Analysis in the Modeling of Non-equilibrium Conditions with a Gas electric Discharge that Simulates the Primary Atmosphere. *Nano engineering*, Vol. 12(30), pp. 3–13 [in Russian].

[Ignatov, Mosin, 2013c](#) – Ignatov, I., Mosin, O.V. (2013c). Structural Mathematical Models Describing Water Clusters. *Journal of Mathematical Theory and Modeling*, 3(11), 72–87.

[Ignatov, Mosin, 2014](#) – Ignatov, I., Mosin, O. V. (2014). The Methods for Studying the Structure of Water Clusters (H<sub>2</sub>O), where n=3-20, Application in Medicine. *Journal of Health, Medicine and Nursing*, Vol. 7, pp. 23-52.

[Ignatov, Mosin, 2014a](#) – Ignatov, I., Mosin, O.V. (2014). Mathematical Models of Distribution of Water Molecules Regarding Energies of Hydrogen Bonds. *Journal of Medicine, Physiology and Biophysics*, 2: 71-94.

[Ignatov, Mosin, 2014b](#) – Ignatov, I., Mosin, O.V. (2014). Mathematical Models Describing Water Clusters as Interaction among Water Molecules. Distributions of Energies of Hydrogen Bonds. *Journal of Medicine, Physiology and Biophysics*, Vol. 3, pp. 48-70.

[Ignatov, Mosin, 2014c](#) – Ignatov, I., Mosin, O. V. (2014). The Methods for Studying the Structure of Water Clusters (H<sub>2</sub>O), where n=3-20. Water Clusters as Nano-structures. *Journal of Health, Medicine and Nursing*, Vol. 8, pp. 29-58.

[Ignatov, Mosin, 2016](#) – Ignatov, I., Mosin, O.V. (2016). Deuterium, Heavy Water and Origin of Life. LAP LAMBERT Academic Publishing, pp. 1-500.

[Ignatov, Mosin, 2016a](#) – Ignatov, I., Mosin, O.V. (2016). Water for Origin of Life Altaspera Publishing & Literary Agency Inc., pp. 1-616.

[Ignatov, Mosin, 2016b](#) – Ignatov, I., Mosin, O.V. (2016). Results of Bioinfluence of Dimitar Risimanski with Biophysical Model Systems, *Journal of Medicine, Physiology and Biophysics*: Vol. 24, pp. 5-17.

**Ignatov, Mosin, 2016c** – Ignatov, I., Mosin, O.V. (2016). Biophysical Results of Bioinfluence of Dimitar Risimanski as Base of Medical Effects. *Journal of Health, Medicine and Nursing*: Vol. 27, pp. 24-35.

**Ignatov, Mosin, 2016d** – Ignatov, I., Mosin, O.V. (2016). Structural Alterations among Water Molecules after Bioinfluence of Dimitar Risimanski. *Advances in Physics Theories and Applications*, Vol. 57, pp. 20-44.

**Ignatov, Tsvetkova, 2011** – Ignatov, I., Tsvetkova, V. (2011). Water for the Origin of Life and “Informationability” of Water, Kirlian (Electric Images) of Different Types of Water. *Euromedica, Hanover*, pp. 62-65.

**Inaba, 1988** – Inaba, H. (1988). Super-high Sensitivity Systems for Detection and Spectral Analysis of Ultraweak Photon Emission from Biological Cells and Tissues. *Experientia*, Vol. 44, pp. 550–559.

**Inaba, 2000** – Inaba, H. (2000). Measurement of biophotons from human body. *J. Int. Soc. Life Inf. Sci.*, 18: 448.

**Kiang et al., 2005** – Kiang, J.G., Ives J.A., Jonas, W.B. (2005). External Bioenergy-induced Increases in Intracellular Free Calcium Concentrations are Mediated by  $\text{Na}^+/\text{Ca}^{2+}$  Exchanger and L-type Calcium Channel. *Mol. Cell Biochem.*, Vol. 271, 51 p.

**Kim, 2002** – Kim, T.J. (2002). Biophoton Emission from Fingernails and Fingerprints of Living Human Subjects. *Acupuncture Electrother Res.*, Vol. 27, 85 p.

**Kirlian, 1949** – Kirlian, S.D. (1949). Method for Receiving Photographic Pictures of Different Types of Objects. USSR Patent № 106401.

**Kwan-Hoong, 2003** – Kwan-Hoong, Ng. (2003). Non-ionizing radiations – Sources, Biological Effects, Emissions and Exposures. *Proceedings of the International Conference on Non-Ionizing Radiation at UNITEN (ICNIR2003). Electromagnetic Fields and Our Health*. 20–22 October 2003.

**Liboff et al., 1984** – Liboff, A.R., Williams, T., Strong, D.M., Wistar, R. (1984). Time-varying Magnetic Fields: Effect on DNA Synthesis. *Science*, Vol. 223, pp. 818–820.

**Marino, 1988** – Marino, A.A. (Ed.) (1988). *Modern Bioelectricity*. Mariele Dekker, New York, Basel.

**Marinov, Ignatov, 2008** – Marinov, M., Ignatov, I. (2008). Color Kirlian Spectral Analysis. Color Observation with Visual Analyzer. *Euromedica, Hanover*, pp. 57-59.

**Marinov, Ignatov, 2008** – Marinov, M., Ignatov, I. (2008). Color Kirlian Spectral Analysis. Color Observation with Visual Analyzer. *Euromedica, Hanover*, pp. 57-59.

**Miller, 1986** – Miller, M.W. (1986). Extremely Low Frequency (ELF) Electric Fields: Experimental Work on Biological Effects. *CRC Handbook of biological effects of electromagnetic fields*, 138–168.

**Mosin, 2011** – Mosin, O.V. (2011). Magnetic Devices for Water Treatment. *C.O.K. Publishing House “Media Technology” (Moscow)*, Vol. 6: 24–27 [in Russian].

**Mosin, 2012** – Mosin, O.V. (2012). Advanced Technologies and Equipment for Magnetic Water Treatment (review). *Water Supply and Sanitary Technique*, Vol. 8: 12–32 [in Russian].

**Mosin, Ignatov, 2015** – Mosin, O.V., Ignatov, I. (2015). An Overview of Methods and Approaches for Magnetic Treatment of Water. *Water: Hygiene and Ecology*, Vol. 3-4 (4): pp. 113-130.

**Motohiro, 2004** – Motohiro, T. (2004). Biophoton Detection as a Novel Technique for Cancer Imaging. *Cancer Science*, Vol. 95(8), pp. 656–661.

**Niggli, 1993** – Niggli, H. (1993). Artificial Sunlight Irradiation Induces Ultra Weak Photon Emission in Human Skin Fibroblasts. *Journal of Photochemistry and Photobiology B: Biology*, Vol. 18 (2–3), pp. 281–285.

**Nikolaev, 2000** – Nikolaev, Y.A. (2000). Distant Interactions in Bacteria. *Microbiology*, Vol. 69(5), pp. 497–503.

**Pehek et al., 1976** – Pehek, J.O., Kyler, H.J., Faust, D.L. (1976). Image Modulating Corona Discharge Photography. *Science*, Vol. 194(4262), pp. 263–270.

**Popp et al., 1992** – Popp, F.A., Li, K., Gu, Q. (1992). Recent Advances in Biophoton Research and its Application, World scientific, 1–18.

**Popp et al., 1994** – Popp, F.A., Quao, G. & Ke-Hsuen, L. (1994). Biophoton Emission: Experimental Background and Theoretical Approaches. *Modern physics Letters B.*, Vol. 8, pp. 21–22.

[Popp et al., 2002](#) – Popp, F.A., Chang, J.J., Herzog, A., Yan, Z. & Yan, Y. (2002). Evidence of Non-classical (squeezed) Light in Biological Systems. *Physics Letters A*, Vol. 293(1–2), pp. 98–102.

[Popp, 2005](#) – Popp, F.A. (2005). Essential Differences Between Coherent and Non-coherent Effects of Photon Emission from Living Organisms. In: X. Shen, R. van Wijk (eds). *Biophotonics*. New York: Springer, 124 p.

[Porter, Wujek, 1988](#) – Porter, N.A., Wujek, D.G. (1988). Reactive Oxygen Species in Chemistry, Biology, and Medicine. In A. Quintanilha, Ed. New York, Plenum Press, pp. 55–79.

[Rattemeyer et al., 1981](#) – Rattemeyer, M., Popp, F.A. & Nagl, W. (1981). Evidence of Photon Emission from DNA in Living Systems. *Nature Wissenshanften*, Vol. 68(11), pp. 572–573.

[Rauhut, 1985](#) – Rauhut, M.M. (1985). Chemiluminescence. In: M. Grayson (Ed). Kirk-Othmer Concise Encyclopedia of Chemical Technology (3rd ed). New York, John Wiley and Sons. 247 p.

[Ring, Hughes, 1986](#) – Ring, E.F.J., Hughes, H. (1986). Real Time Video Thermography in Recent Developments in Medical and Physiological Imaging. *Suppl. Journal of Medical Engineering and Technology*, pp. 86–89.

[Rubik, 2002](#) – Rubik, B. (2002). The biofield hypothesis: its biophysical basis and role in medicine. *J. Altern. Complement Med.*, Vol. 8(6), pp. 703–717.

[Sessler, Gerhard-Multhaupt, 1998](#) – Sessler, G.M., Gerhard-Multhaupt, R. (eds) (1998). Electrets. *Laplacian Press, Morgan Hill, California, USA*.

[Seto et al., 1992](#) – Seto, A., Kusaka, C. Nakazato, S. et al. (1992). Detection of Extraordinary Large Bio-magnetic Field Strength from Human Hand. *Acupuncture Electrother Res. Int. J.*, Vol. 17, 75 p.

[Shimizu et al., 1995](#) – Shimizu H., Suzuki, Y., Okonogi, H. (1995). Biological Effects of Electromagnetic Fields. *Nippon Eiseigaki Zasshi.*, Vol. 50(6), pp. 919–931.

[Sisodia, 2007](#) – Sisodia, M.L. (2007). Microwaves: Introduction to Circuits, Devices and Antennas. *New Delhy, New Age International Ltd.*, 602 p.

[Vladimirov, 1996](#) – Vladimirov, Y.A. (1996). Studies of Antioxidants with Chemiluminescence. In: *Proceedings of the International Symposium on Natural Antioxidants. Molecular Mechanisms and Health Effects*. L. Packer, M.G. Traber & W. Xin (eds.), pp. 125–144.

[Wikswow, Barach, 1980](#) – Wikswow, J., Barach, J. (1980). An Estimation of the Steady Magnetic Field Strength Required to Influence Nerve Condition. *IEEE Trans. Bio-Med. Eng.*, Vol. 27, pp. 722–723.

[Young, Roper, 1976](#) – Young, R.E., Roper, C.F. (1976). Bioluminescent Countershading in Midwater Animals: Evidence from Living Squid. *Science*, Vol. 191(4231), pp. 1046–1048.

[Zhadin, 2001](#) – Zhadin, M.N. (2001). Review of Russian Literature on Biological Action of DC and Low-frequency AC magnetic fields. *Bioelectromagnetics*, Vol. 22, pp. 27–45.

[Zlatkevich, Kamal-Eldin, 2005](#) – Zlatkevich, L., Kamal-Eldin, A. (2005). Analysis of Lipid Oxidation. In: A. Kamal-Eldin & J. Pokorn (Eds.). New York, AOCS Publishing, 281 p.

Copyright © 2017 by Academic Publishing House Researcher s.r.o.



Published in the Slovak Republic  
European Journal of Medicine  
Has been issued since 2013.  
ISSN: 2308-6513  
E-ISSN: 2310-3434  
2017, 5(2): 56-63

DOI: 10.13187/ejm.2017.2.56  
[www.ejournal5.com](http://www.ejournal5.com)



## Action of Cytisinum on the Transport Mediators and Calcium Channel of Glutamatergic Neurotransmitter Systems of the NMDA Receptor

Nozim N. Khoshimov<sup>a,\*</sup>, K.E. Nasirov<sup>a</sup>

<sup>a</sup>A.S. Sadikov Institute of Bioorganic Chemistry,  
Academy of Sciences of the Republic of Uzbekistan, Republic of Uzbekistan

### Abstract

**Background:** The purpose of this study was the effect of the alkaloid Cytisinum regulation of the calcium channels of brain synaptosomes in rats. This enables the regulation of the transport of mediator's glutamatergic neurotransmitter receptors.

**Methods:** The study was carried out using the Weilers method. Synaptosomes were isolated from the brain of rats by a two-step centrifugation method. The entire isolation procedure was carried out at 4°C. To measure the amount of cytosolic Ca<sup>2+</sup> synaptosomes were calculated by the Grinkevich equation.

**Results:** Increase in the concentration of Ca<sup>2+</sup> ([Ca<sup>2+</sup>]<sub>i</sub>) caused by glutamate, primarily due to activation of membrane permeability, movement of Ca<sup>2+</sup> into the cell and release of Ca<sup>2+</sup> from intracellular stores. Cytisinum does not compete with glutamate for the binding site. Perhaps the effect of Cytisinum is due to the interaction with the ion channels of NMDA receptors. Cytisinum is able to interact with the glutamate binding site of the NMDA receptor and allosteric modulating sites located on the membrane of the ion channels. In these studies it was shown that in the presence of Cytisinum, the inhibitory effect of magnesium ions (10 μM) is not observed. This is probably due to competition between Mg<sup>2+</sup> and Cytisinum over sites that stimulate the opening of ion channels. Perhaps there is a competition between Cytisinum and nifedipine for the site of regulation of dihydropyridine-sensitive calcium channels.

**Conclusion:** The action of the alkaloid of Cytisinum is due to the interaction with the ion channels of NMDA receptors. Cytisinum is able to interact with the glutamate binding site of the NMDA receptor and the allosteric modulating sites. There is competition between Mg<sup>2+</sup> and Cytisinum over sites that stimulate the opening of ion channels and in nifedipine for the site of regulation of dihydropyridine-sensitive calcium channels.

**Keywords:** synaptosomes, NMDA, glutamate, Cytisinum, nifedipine, Mg<sup>2+</sup>.

### 1. Introduction

NMDA receptors (NMDARs) are glutamate-gated cation channels with high calcium permeability that play important roles in many aspects of the biology of higher organisms. They are

\* Corresponding author

E-mail addresses: [nozimka@inbox.ru](mailto:nozimka@inbox.ru) (N. Khoshimov)

critical for the development of the central nervous system (CNS), generation of rhythms for breathing and locomotion, and the processes underlying learning, memory, and neuroplasticity. Consequently, abnormal expression levels and altered NMDAR function have been implicated in numerous neurological disorders and pathological conditions. NMDAR hypofunction can result in cognitive defects, whereas overstimulation causes excitotoxicity and subsequent neurodegeneration. Therefore, NMDARs are important therapeutic targets for many CNS disorders (Kemp et al., 2002; Jansen et al., 2003; Chazot, 2004; Farlow, 2004; Wood, 2005; Cai, 2006; Missale et al., 2006; Brown et al., 2006) including stroke, hypoxia, ischemia, head trauma, Huntington's, Parkinson's, and Alzheimer's diseases, epilepsy, neuropathic pain, alcoholism, schizophrenia, and mood disorders. To date, drugs targeting NMDARs have had only limited success clinically due to poor efficacy and unacceptable side effects, including hallucinations, catatonia, ataxia, nightmares, and memory deficits.

A detailed understanding of the mechanisms underlying agonist-induced receptor activation would facilitate development of more selective drugs that target specific NMDAR subtypes and alter their function to a well-defined extent. This chapter will investigate the physiological roles NMDARs play in the mammalian nervous system and the molecular and structural basis of NMDAR activation. One of the main questions that will be addressed is how agonist binding results in opening of the NMDAR ion channel. Although the mechanism coupling ligand binding to channel opening remains incompletely understood for NMDARs, we propose that this process suggests promising approaches to drug design (Antonius et al., 2008).

Glutamate is the major excitatory neurotransmitter, in the mammalian CNS. Not surprising, then, that a large number of physiological functions based on the active use of glutamatergic transmission. It would be impractical to try to describe all the possible physiological effects of the activation of the NMDA-receptor complex. Nevertheless, there are three main physiological functions of NMDA-receptor, which reflect the functional characteristics of these receptors are the basis for the development of pharmacological modulation techniques.

In light of this, special attention attracts glutamatergic system of the brain. The glutamatergic system includes receptors (ionotropic and metabotropic) glutamate and carriers. signal feature in the synapse by means of glutamate is that in addition to neurons in the process are directly involved glial cells: as for the termination of the exciting action of glutamate needed its evacuation from the synaptic cleft, glutamate is transferred into astrocytes, where "neutralized", turning into glutamine (Cycle glutamate/glutamine works much more intense, "reuptake" torus neurotransmitters glutamate neural carriers).

In the pathology, Nicholson et al (Nicholson et al., 1977) showed that hypoxia of the brain tissue causes a rapid increase in the concentration of intracellular calcium in them, the "calcium hypothesis" was transferred to brain neurons to explain calcium-mediated neuronal death in ischemia/hypoxia, hypoglycemia, and epilepsy (Siesjo, 1994). And after the culture of neurons (Rothman et al., 1987) and brain sections (Garthwaite et al., 1986) showed that glutamate and the corresponding excitatory amino acids cause neuronal cell death, the name "excitatory glutamate toxicity" arose. Currently, the hypothesis of "glutamate excitotoxicity" in most cases is considered within the "calcium hypothesis of ischemic cell death" (Kristian et al., 1998). Its main provisions in the application to the tissues of the brain are as follows.

The concentration of free  $\text{Ca}^{2+}$  in the cytoplasm of cells is about  $10^{-7}$  M, while in the intercellular environment and in the cellular organelles it is about  $10^{-3}$  M. As a result of ATP deficiency, the activity of active calcium transporters (Ca-ATPase and Na / Ca-exchangers) decreases The  $\text{Ca}^{2+}$  concentration in the cytoplasm increases. In addition, the deficiency of ATP leads to a decrease in the membrane potential, which in turn activates the potential-dependent Ca channels, and this leads to an even greater increase in the intracellular  $\text{Ca}^{2+}$  concentration.

Because of the specific nature of nerve cells, a fatal role in them is played by an increase in the concentration of  $\text{Ca}^{2+}$  in the presynapses region, which leads to a massive release of various neurotransmitters, among which the exciting mediator glutamic acid has a special role. This is due to the fact that, first of all, the most synapses in the brain (about 40%) are glutamate-ergic and, secondly, the majority of postsynaptic glutamate receptors (NMDA- and AMPA-receptors) control the calcium channels and, correspondingly, even more Increase the concentration of intracellular  $\text{Ca}^{2+}$ . In connection with this positive feedback, the concentration of cytoplasmic  $\text{Ca}^{2+}$  in glutamate-sensitive neurons increases dramatically. Therefore, up to now, one more name of the processes

occurring in the ischemic focus of the brain continues to exist: "exciting toxicity" or otherwise "glutamate excitotoxicity" (Kristian et al., 1998; Fohr et al., 1995; Berridge, 1993).

Like other divalent cations  $\text{Ca}^{2+}$  have a negative modulatory influence on the activity of NMDA-receptor complex. High extra- and intracellular  $\text{Ca}^{2+}$  concentration reduces the NMDA-receptor channel conductivity (McBain et al., 1994), which can be seen as paradoxical, but very reasonable self-defense mechanism of the neuron from overstimulation. The inhibitory effect of  $\text{Ca}^{2+}$  could be due to redistribution of the surface charge of the membrane with a specific blocking action ("blockage of the channel"), activation of tyrosine and serine phosphatases that dephosphorylate C-terminal fragments of subunits  $\text{NR}_1$  and  $\text{NR}_2$ , activation of calmodulin, NO-synthetase, as well as depolymerization of actin.

The modulating effect of  $\text{Ca}^{2+}$  may be mediated by changes in the cytoskeleton. For example, it was found that the activity of NMDA-receptor complex aktinopodobnym regulated protein that is depolymerized by increasing intracellular calcium concentration (Rosenmund et al., 1993) It is believed that the  $\text{Ca}^{2+}$ -dependent inactivation of NMDA-receptor complex occurs with the participation of several regulatory proteins -  $\alpha$ -actinin-2 neurofilament- a (Ehlers et al., 1998), as well as postsynaptic PSD family of proteins that bind to the subunits  $\text{NR}_2$  (Harris et al., 1997). The meaning of this regulation is that the NMDA-receptor (more precisely, its channel) is active only when the regulatory proteins bind subunits klasterizuya receptor complex in the synaptic region in close proximity to second messenger systems Clustering is another highly efficient mechanism of self-regulation activity NMDA-receptor complex, since the entrance of  $\text{Ca}^{2+}$  through the channel associated with the NMDA-receptor, promotes inactivation of receptors due to activation of  $\text{Ca}^{2+}$  -dependent phosphatase, calmodulin, which prevent binding of NMDA-receptor complex ( $\text{NR}_1$  subunit) with elements of the cytoskeleton (Rosenmund et al., 1993; Ehlers et al., 1998).

Purpose: Actions on glutamatergic neurotransmitter system of the NMDA-receptor.

Tasks:

- Study of Cytisinum effect on binding site agonist (glutamate).
- The study of Cytisinum acts on the glycine co-agonist binding site.
- Study on the action of Cytisinum binding site  $\text{Mg}^{2+}$ .
- The study of Cytisinum binding site of action in the "channel" blockers.

## 2. Material and methods

Experiments were conducted on 20 outbred male albino rats weighing (200-250 g) contained in a standard vivarium ration. All experiments were performed in accordance with the requirements of "the World Society for the Protection of Animals" and "European Convention for the protection of experimental animals" (European Convention..., 1986). Synaptosomes isolated from rat brain by a two-step centrifugation (Weiler et al., 1981). The whole procedure of selection was carried out at 4°C. To measure the amount of cytosolic  $\text{Ca}^{2+}$  was calculated from the equation of Grinkevich (Gryniewicz et al., 1985) in synaptosomes isolated from brain of rats placed in an environment similar to, the one that was used to isolate cells were added 20  $\mu\text{M}$  of chlortetracycline (CTC). Incubated for 60 min to achieve maximal interaction with the membrane – CTC  $\text{Ca}^{2+}$  as in plasma, and intracellular membranes. CTC excitation wavelength – 405 nm, recording – 530 nm. Results are expressed as a percentage, taking 100 % of the difference between the maximum value of fluorescence intensity (fluorescence dye, a saturated  $\text{Ca}^{2+}$ ) and its minimum value (in the absence of fluorescence of the indicator of  $\text{Ca}^{2+}$ ) obtained after adding ethylene-glycol-bis-amino-ethyl-tetra-acetate EGTA.

Statistical analysis

The measurements were made using a universal spectrometer (USB-2000). Statistical significance of differences between control and experimental values determined for a number of data using a paired t-test, where the control and the experimental values are taken together, and unpaired t-test, if they are taken separately. The value of  $P < 0.05$  indicated a statistically significant differences.

The results obtained are statistically processed to Origin 6.1 (Origin Lab Corporation, USA).

### 3. Results and discussion

Action alkaloid Cytisinum (*1R, 5S*)-1,2,3,4,5,6-hexahydro-1,5-methano-8H-pyrido [1,2a] [1,5] diazocin-8-one, isolated from plants (*Thermopsis lanceolata* R. Br and *Cytisus ruthenicus*) on cytosolic  $\text{Ca}^{2+}$  in brain synaptosomes of rats.

In the experiments the influence of glutamate on intracellular calcium level was investigated in synaptosomes from rat brain. Pre using the  $\text{Ca}^{2+}$ -sensitive chlortetracycline (CTC) set ratio of fluorescence excited by light having wavelengths of 340 and 380 nm ( $F_{340}/F_{380}$ ) in synaptosomes. When removing  $\text{Ca}^{2+}$  from the extracellular medium, pre-incubation of EGTA resulted in a decrease in fluorescence at 5 %. In the presence of EGTA in the incubation medium, glutamate at concentrations of 1-100  $\mu\text{M}$  dose-dependent increases in fluorescence level at 25-48 %, which indicates an increase in the concentration of cytosolic  $\text{Ca}^{2+}$  ( $[\text{Ca}^{2+}]_i$ ), called glutamate, primarily due to activation of membrane permeability movement of  $\text{Ca}^{2+}$  into the cell and release of  $\text{Ca}^{2+}$  from intracellular stores (Fig. 1).

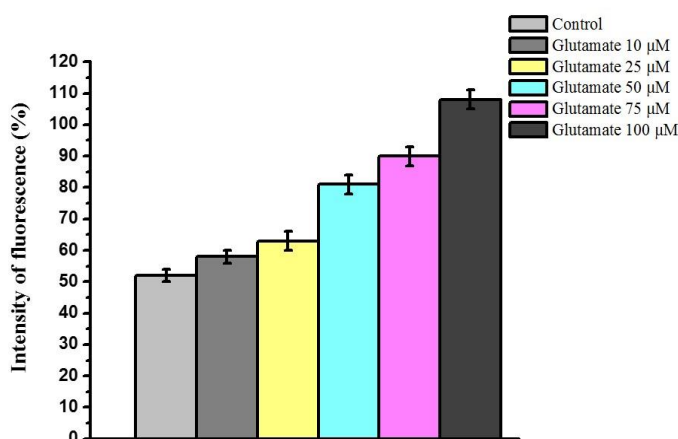


**Fig. 1.** The dose-dependent effect of glutamate on the level of fluorescence. Reliability index  $P < 0.05$

Pre-incubation of the alkaloid Cytisinum reduced fluorescence and therefore the level of cytosolic calcium under the action of glutamate at the complex CTC-synaptosomes (Fig. 2).

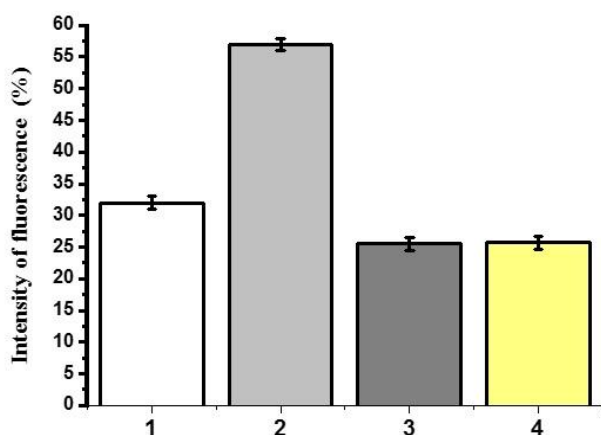


**Fig. 2.** Influence of the alkaloid Cytisinum in the glutamatergic neurotransmitter system

- 1 - fluorescence control complex CTC-synaptosomes;
- 2 - fluorescence complex CTC-synaptosomes by adding 50  $\mu\text{M}$  glutamate;
- 3 - adding 50  $\mu\text{M}$  glutamate in the background Cytisinum.
- 4 - Cytisinum 50  $\mu\text{M}$ . Reliability index  $P < 0.05$ .

In studying the action alkaloid Cytisinum rat brain synaptosomes found that alkaloid Cytisinum significantly reduces the fluorescence, respectively cytosolic calcium levels compared to the control. At the same time increase the concentration of Cytisinum from 10 to 100  $\mu\text{M}$  glutamates for background did not lead to further reduction of the effect of glutamate.

The results show that alkaloid Cytisinum does not compete with the binding site for glutamate. Perhaps the action of Cytisinum has interaction with ion channels of NMDA-receptors.

It is known that,  $\text{Mg}^{2+}$  ions selectively block the activity of NMDA receptors. Glycine enhances NMDA-receptor responses, increasing the frequency of channel opening. In the complete absence of glycine receptor is not activated by L-glutamate.

Indeed, adding to the incubation medium increased the 5  $\mu\text{M}$  glycine-glutamate-dependent fluorescence increase by 15-20 %. At the same time the ions  $\text{Mg}^{2+}$  (50  $\mu\text{M}$ ) inhibited the glutamate-induced  $\text{Ca}^{2+}$  release from intracellular stores (Fig. 3).

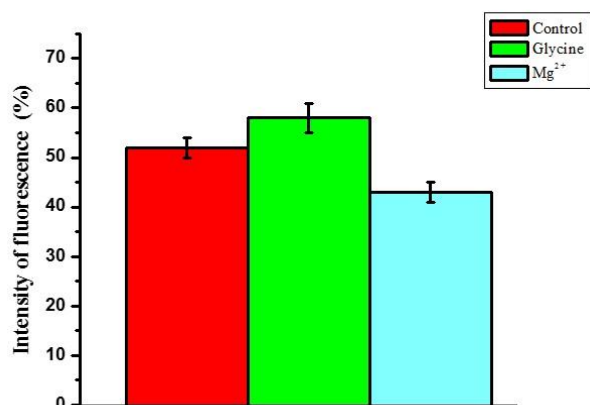


**Fig. 3.** The action of glycine and  $\text{Mg}^{2+}$  ions to glutamate-induced intracellular  $\text{Ca}^{2+}$  stores. Reliability index  $P < 0.05$

It is known that glycine stimulating effects of glutamate and competitive receptor antagonists such as  $\text{AP}_5$ , AV-2-1 toxin can prevent activation of glutamate. Other drugs and  $\text{Mg}^{2+}$  ions may block the open channel through the non-competitive antagonism. These medications include experimental neuroprotective drug MK-801 and argiobate (Martin et al., 1977).

In order to identify, possible interaction with Cytisinum areas overstimulation NMDA-receptor responsible for the opening of calcium channels, investigated its effect on the background of the non-competitive antagonists such as magnesium ions, argiobate and calcium channel blockers – nifedipine.

It is shown that magnesium ions in mill molar concentrations significantly inhibit the fluorescence of the complex glutamate CTC-synaptosomes. The inhibitory effect of magnesium ions fluorescence complex CTC-synaptosomes in the presence of Cytisinum is not changed.

These studies have shown that in the presence of Cytisinum inhibitory effect of magnesium ions (10  $\mu\text{M}$ ) was observed. This is probably due to the competition between the  $\text{Mg}^{2+}$  and Cytisinum for sites that promote opening of ion channels. Also, shown that argiobate effect on NMDA-receptor calcium channels in the presence of Cytisinum is not changed (Fig. 4).



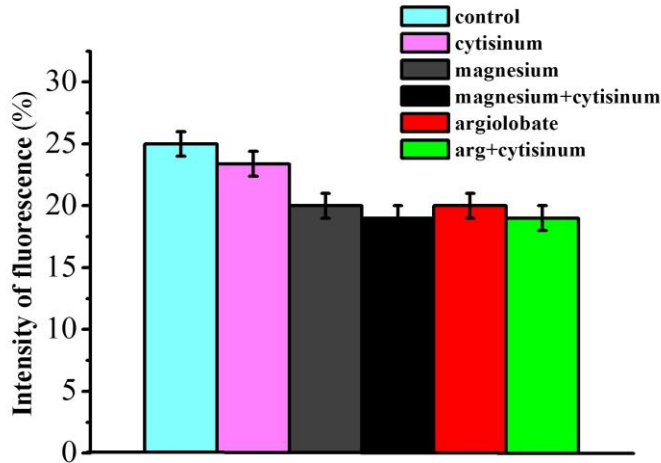


**Fig.4.** The effect of magnesium ions and Cytisinum at argiolobate fluorescence and cytosolic calcium levels in rat brain synaptosomes. Reliability index  $P < 0.05$ .

In studying the action of Cytisinum for calcium-dependent processes are NMDA-receptor were examined for background nifedipine ( $\text{Ca}^{2+}$  channel blocker of L-type) in synaptosomes from rat brain.

Pre-incubation of nifedipine with CTC synaptosomes-complex, led to a decrease in fluorescence. Pre-incubation with Cytisinum CTC synaptosomes-complex, also led to a decrease in fluorescence. Pre-incubation of Cytisinum in the background with nifedipine CTC synaptosomes-complex, led to a slight decrease in fluorescence (Fig. 5), which indicates that competition between Cytisinum and nifedipine for land regulation dihydropyridine-sensitive calcium channels.

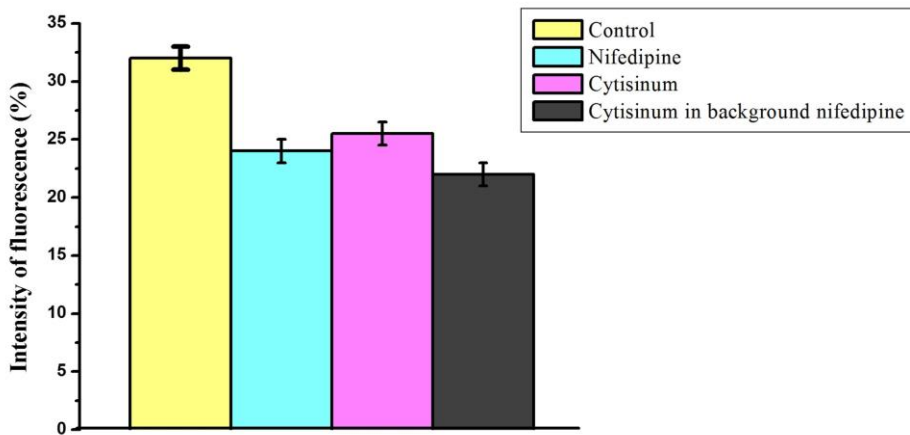


**Fig. 5.** Effect of Cytisinum for calcium-dependent processes on NMDA-receptor in background nifedipine. Reliability index  $P < 0.05$

These results demonstrate the possibility of use in the regulation of Cytisinum dihydropyridine-sensitive calcium channel subtypes major neuronal receptors.

#### 4. Conclusions

Increase in the concentration of cytosolic  $\text{Ca}^{2+}$  ( $[\text{Ca}^{2+}]_i$ ), called glutamate, primarily due to activation of membrane permeability, movement of  $\text{Ca}^{2+}$  into the cell and release of  $\text{Ca}^{2+}$  from intracellular stores. Cytisinum does not compete for the glutamate binding site. Perhaps the action of Cytisinum has the interaction with ion channels, NMDA-receptors. The Cytisinum capable of interacting with the glutamate binding site of the NMDA-receptor sites allosterically modulate

disposed on a membrane ion channel. These studies have shown that in the presence of Cytisinum inhibitory effect of magnesium ions (10  $\mu\text{M}$ ) was not observed. This is probably due to the competition between the  $\text{Mg}^{2+}$  and Cytisinum for sites that promote opening of ion channels. There may be competition between Cytisinum and nifedipine for land regulation dihydropyridine-sensitive calcium channels.

As in any field of fundamental science, the completion of one stage does not solve all problems. In what directions can we continue to develop the results and conclusions of this work. First, it is necessary to continue the research of substances for which effects on these channels are found: pharmaceutical preparations and alkaloids. Secondly, it is necessary to continue the search for resonance frequencies for other physiologically significant ions:  $\text{Na}^+$ ,  $\text{K}^+$ ,  $\text{Cl}^-$ ,  $\text{Fe}^{2+}$ , GABA, acetylcholine, etc., and to explore the possibility of simultaneous application of several frequencies to activate various processes in the body.

## References

- European Convention..., 1986 – European Convention for the Protection of Vertebrate Animals used for Experimental and other Scientific Purposes. Strasbourg. 1986. Available from: <http://conventions.coe.int>
- Ehlers et al., 1998 – Ehlers, M.D., Fung, E.T., O'brien, R.J., Haganir, R.L. (1998). Splice variant-specific interaction of the NMDA receptor subunit  $\text{NR}_1$  with neuronal intermediate filaments//*J. Neurosci.* Vol. 18.P. 720-730.
- Grynkiewicz et al., 1985 – Grynkiewicz G., Poenie M., Tsien R.Y. (1985). A new generation of  $\text{Ca}^{2+}$ , indicators with greatly improved fluorescence properties. *J. Biol. Chem.*, Vol. 260, pp. 3440–3450.
- Harris et al., 1997 – Harris, R.A, Mihic, S. J., Brozowski, S., Hadmgham, K., Whiting, P. J. (1997). Ethanol, flumtrazepam, and pentobarbital modulation of  $\text{GABA}_A$  receptors expressed in mammalian cells and *Xenopus* oocytes. *Alcohol Chn Exp Res.*, Vol. 21, pp. 444-451.
- Martin et al., 1977 – Martin, W.R., Sloan, J.W. (1977). Pharmacology and classification of LSD-like hallucinogens. In W. R. Martin (Ed.), *Drug addiction II* (P. 305-368). New York: Springer-Verlag.
- McBain et al., 1994 – McBain, C.J., Mayer, M.L. (1994). N-methyl-D-aspartate receptor structure and function. *Physiol. Rev.* Vol.74, pp. 723-760.
- Rosenmund et al., 1993 – Rosenmund, C. Westbrook, G.L. (1993). Calcium-induced actin depolymerization reduces NMDA channel activity. *Neuron* 10. pp. 805–814.
- Weiler et al., 1981 – Weiler, M.H., Gundersen, C.B., Jenden, D.J. (1981). Choline uptake and acetylcholine synthesis in synaptosomes: Investigations using two differently labelled variants of choline. *Neurochem.* 36, pp. 1802-1812.
- Nicholson et al., 1977 – Nicholson, C, Bruggencate, G.T., Steinberg, R., Stockle, H. (1977). Calcium modulation in brain extracellular microenvironment demonstrated with ion-selective micropipette. *Proc Nat Acad Sci U S A.* V. 74, pp. 1287–1290.
- Rothman et al., 1987 – Rothman, S.M., Olney, J.W. (1987). Excitotoxicity and the NMDA receptor. *Trends Neurosci.*, V.10. pp. 299–302.
- Siesjo, 1994 – Siesjo, B.K. (1994). Cell damage in the brain: a speculative synthesis. *J Cereb Blood Flow Metab.*, V.1. pp. 155–185.
- Garthwaite et al., 1986 – Garthwaite, G, Garthwaite, J. (1986). Neurotoxicity of excitatory amino acid receptor agonists in rat cerebral slices: dependence on calcium concentration. *Neurosci Lett.* V.66, pp. 193–198.
- Kristian et al., 1998 – Kristian, T., Siesjo, B.K. (1998). Calcium in ischemic cell death. *Stroke.* V.29, pp. 705-718.
- Fohr et al., 1995 – Fohr, K.J., Mayerhofer, A., Gratzl, M. (1995). Control of intracellular free calcium in neurons and endocrine cells. NATO ASI Series. *Trafficking of Intracellular Membranes.* Springer-Verlag Berlin Heidelberg. V. H 91. pp. 303–313.
- Berridge, 1993 – Berridge, M.J. (1993). Inositol trisphosphate and calcium signaling. *Nature.* V.361, pp. 315-325.
- Kemp et al., 2002 – Kemp, J.A, McKernan, R.M. (2002). NMDAR pathways as drug targets. *Nature Neurosci.*, 5: 1039.

[Jansen et al., 2003](#) – Jansen, M, Dannhardt, G. (2003). Antagonists and agonists at the glycine site of the NMDAR for therapeutic interventions. *Eur J Med Chem.*, 38: 661.

[Chazot, 2004](#) – Chazot, P.L. (2004). The NMDAR NR2B subunit: a valid therapeutic target for multiple CNS pathologies. *Curr Med Chem.*, 11: 389.

[Farlow, 2004](#) – Farlow, M.R. (2004). NMDAR antagonists. A new therapeutic approach for Alzheimer's disease. *Geriatrics*, 59: 22.

[Wood, 2005](#) – Wood, P.L. (2005). The NMDAR complex: a long and winding road to therapeutics. *IDrugs*, 8: 229.

[Cai, 2006](#) – Cai, S.X. (2006). Glycine/NMDAR antagonists as potential CNS therapeutic agents: ACEA-1021 and related compounds. *Curr. Topics Med. Chem.*, 6, 651.

[Missale et al., 2006](#) – Missale, C. et al. (2006). The NMDA/D<sub>1</sub> receptor complex as a new target in drug development. *Curr Topics Med Chem.*, 6: 801.

[Brown et al., 2006](#) – Brown, D.G, Krupp, J.J. (2006). N-methyl-D-aspartate receptor (NMDA) antagonists as potential pain therapeutics. *Curr Topics Med Chem.*, 6: 749.

[Antonius et al., 2008](#) – VanDongen, Antonius M. J., Blanke, Marie L. (2008). Activation Mechanisms of the NMDA Receptor. *J. Biology of the NMDA Receptor*. pp. 283–312.